HHS Public Access

Author manuscript

Eur J Neurosci. Author manuscript; available in PMC 2017 August 01.

Published in final edited form as:

Eur J Neurosci. 2016 August ; 44(3): 2015–2027. doi:10.1111/ejn.13288.

Mechanisms, pools, and sites of spontaneous vesicle release at synapses of rod and cone photoreceptors

Karlene M. Cork[1,2], **Matthew J. Van Hook**[1], and **Wallace B. Thoreson**[1,2]

[1]Truhlsen Eye Institute, Department of Ophthalmology & Visual Sciences, University of Nebraska Medical Center, Omaha, NE, USA

[2]Department of Pharmacology and Experimental Neuroscience, University of Nebraska Medical Center, Omaha, NE, USA

Abstract

Photoreceptors have depolarized resting potentials that stimulate calcium-dependent release continuously from a large vesicle pool but neurons can also release vesicles without stimulation. We characterized the Ca^{2+} dependence, vesicle pools, and release sites involved in spontaneous release at photoreceptor ribbon synapses. In whole cell recordings from light-adapted horizontal cells (HCs) of tiger salamander retina, we detected miniature excitatory post-synaptic currents (mEPSCs) when no stimulation was applied to promote exocytosis. Blocking Ca^{2+} influx by lowering extracellular Ca^{2+}, by application of Cd^{2+} and other agents reduced the frequency of mEPSCs but did not eliminate them, indicating that mEPSCs can occur independently of Ca^{2+}. We also measured release presynaptically from rods and cones by examining quantal glutamate transporter anion currents. Presynaptic quantal event frequency was reduced by Cd^{2+} or by increased intracellular Ca^{2+} buffering in rods, but not in cones, that were voltage-clamped at −70 mV. By inhibiting the vesicle cycle with bafilomycin, we found the frequency of mEPSCs declined more rapidly than the amplitude of evoked EPSCs suggesting a possible separation between vesicle pools in evoked and spontaneous exocytosis. We mapped sites of Ca^{2+}-independent release using total internal reflectance fluorescence (TIRF) microscopy to visualize fusion of individual vesicles loaded with dextran-conjugated pHrodo. Spontaneous release in rods occurred more frequently at non-ribbon sites than evoked release events. The function of Ca^{2+}-independent spontaneous release at continuously active photoreceptor synapses remains unclear, but the low frequency of spontaneous quanta limits their impact on noise.

Graphical Abstract

Photoreceptors have depolarized resting potentials that stimulate continuous Ca^{2+}-dependent release. We found evidence for Ca^{2+}-dependent spontaneous release in strongly hyperpolarized rods when Ca^{2+} channels should be minimally active and Ca^{2+}-independent spontaneous release that persisted after blocking Ca^{2+} influx in both rods and cones. Ca^{2+}-independent spontaneous release from rods occurred more often at ectopic sites than evoked release which clusters near ribbon-style active zones.

Corresponding Author, Dr. Wallace B. Thoreson, Department of Ophthalmology and Visual Sciences, 4050 Durham Research Center, University of Nebraska Medical Center, Omaha, NE 68198-5840, Fax #- 402-559-5368, wbthores@unmc.edu.

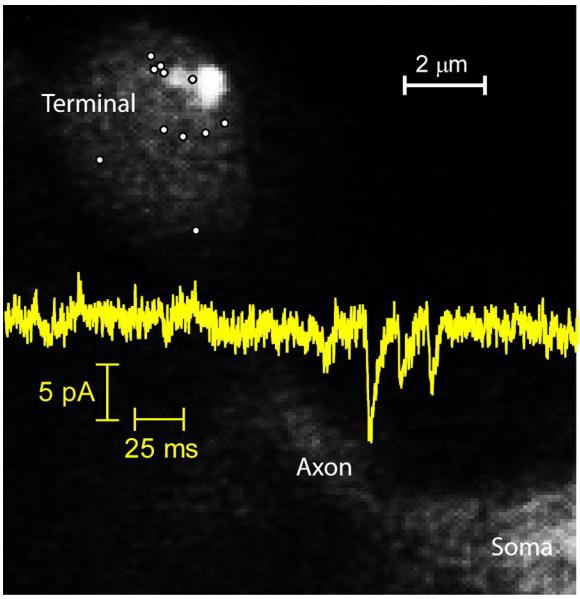

Keywords

Exocytosis; retina; calcium; ribbon synapse; spontaneous synaptic release; tiger salamander

Introduction

Neurons transmit signals by the evoked release of vesicles, triggered by cell depolarization and resultant opening of voltage-gated Ca^{2+} channels (Katz, 1969; Llinás, 1991; Schweizer & Ryan, 2006). In photoreceptors, release is regulated by the opening of L-type Ca^{2+} channels clustered beneath protein structures known as synaptic ribbons (Nachman-Clewner et al., 1999; Morgans, 2001; Mercer et al., 2011; Bartoletti et al., 2011; Van Hook & Thoreson, 2015). Neurons are also capable of spontaneous release that does not require depolarization. The functions and mechanisms of spontaneous release are not as well understood as those of evoked release and appear to vary among synapses (see reviews by Kaeser & Regehr, 2014; Kavalali, 2015; Schneggenburger & Rosenmund, 2015).

Postsynaptic properties of HC mEPSCs have been characterized in a number of species (Maple et al., 1994; Hirasawa et al., 2001; Cadetti et al., 2005; Feigenspan & Babai, 2015), but there has been limited study of the presynaptic mechanisms regulating spontaneous release from photoreceptors. Because photoreceptors maintain relatively depolarized membrane potentials allowing continuous Ca^{2+} channel activity, we considered that perhaps all spontaneous mEPSCs from photoreceptors might arise from Ca^{2+}-dependent release. However, spontaneous mEPSCs have been found to persist in retinal HCs in the presence of Co^{2+} under nominally Ca^{2+}-free conditions (Maple et al., 1994) suggesting a possible contribution from Ca^{2+}-independent spontaneous release. Because functionally significant Ca^{2+} currents can also persist in photoreceptors under these conditions (Piccolino et al., 1996, 1999; Piccolino & Pignatelli, 1996), we confirmed and extended these conclusions using additional blockers. In addition to measuring mEPSCs postsynaptically, we measured

spontaneous release presynaptically in photoreceptors by recording anion currents associated with glutamate transporter activity. This allowed us to distinguish spontaneous release from rods and cones and to determine if differences in mEPSCs were due to presynaptic or postsynaptic effects. The question of whether vesicle pools involved in spontaneous release overlap with pools involved in evoked release has been the subject of vigorous debate (Kaeser & Regehr, 2014; Kavalali, 2015; Schneggenburger & Rosenmund, 2015). Ribbon-style synapses possess larger and more mobile vesicle pools than conventional synapses (Rea et al., 2004; Holt et al., 2004) and we also asked whether these vesicle pools overlap in photoreceptor synapses. Finally, we determined whether spontaneous release occurs at the same sites or different sites from evoked release.

Our experiments determined that there are three forms of basal release from rods and cones: 1) Ca^{2+}-dependent, evoked release driven by the voltage-dependent activation of L-type Ca^{2+} channels, 2) Ca^{2+}-dependent spontaneous release that occurs at negative membrane potentials where Ca^{2+} channels should be inactive, and 3) Ca^{2+}-independent spontaneous release that persists after inhibiting Ca^{2+} influx. Ca^{2+}-independent spontaneous release events in rods occurred more often than evoked release at non-ribbon sites. The frequency and amplitude of mEPSC events declined more rapidly in the presence of a vesicular ATPase inhibitor than the amplitude of evoked EPSCs, consistent with a possible separation of vesicle pools involved in evoked and spontaneous release.

Materials and methods

Retinal slice

Retinal slice preparations were made using the retinae from 55 aquatic tiger salamanders (*Ambystoma tigrinum*; both sexes, 18–25 cm length; Charles Sullivan, Nashville, TN) following methods described by Van Hook and Thoreson (2013). The University of Nebraska Medical Center's Institutional Animal Care and Use Committee approved all experimental procedures. Salamanders were housed in a tank of water maintained at 4–8 °C on a 12 h:12 h light-dark cycle. Salamanders are sacrificed 1–2 hours into the dark cycle following treatment with 0.25 g/L MS222 for 15 minutes. The eyes were then enucleated and the anterior segment and lens were both removed. A section of eyecup was placed vitreal side down onto a nitrocellulose membrane (5 × 10 mm; type AAWP, 0.8 μm pores; Millipore). The sclera, choroid and retinal pigment epithelium were gently separated from the retina in cold amphibian saline solution to isolate the retina. A razor blade tissue slicer (Stoelting Co.) was used to cut the isolated retina into 125-μm slices, which were then rotated 90 degrees and anchored to the recording chamber with vacuum grease. Dissections were performed under room lights. Retinal slices were visualized on an upright fixed-stage microscope (E600FN; Nikon) equipped with a long-working distance 60X (1.0 NA) water-immersion objective. The tissue was superfused at ~1 ml/min with an oxygenated amphibian saline solution containing the following (in mM): 111 NaCl, 2.5 KCl, 1.8 $CaCl_2$, 0.5 $MgCl_2$, 5 glucose, and 10 HEPES (pH 7.8; 240–245 mOsm). A 0 Ca^{2+} extracellular solution was prepared by adding 1 mM EGTA to a Ca^{2+}-free extracellular solution in order to buffer any residual Ca^{2+}.

Electrophysiology and mEPSC analysis

Whole-cell patch clamp recordings from post-synaptic horizontal cells (HCs) were made using the retinal slice preparation described above. Patch pipettes with tip diameters of 1–2 μm were pulled from borosilicate glass (1.2 mm outer diameter, 0.9 mm inner diameter, with internal filament; World Precision Instruments) on a Narishige PP-830 vertical puller. Pipettes had resistances of 12–20 MΩ when filled with a solution containing the following (in mM): 40 Cs glutamate, 50 Cs gluconate, 10 TEACl, 3.5 NaCl, 1 $CaCl_2$, 1 $MgCl_2$, 10 MgATP, 0.5 GTP, 5 EGTA, and 10 HEPES (pH 7.2; 235–240 mOsm). Huxley-Wall micromanipulators were used to position pipettes such that the tip contacted the cell body, which was identified morphologically and from its position in the retinal layers. Once a giga-ohm seal was formed, gentle suction was used to rupture the patch. HCs were voltage clamped at −60 mV with a Multiclamp 700A amplifier (Axon Instruments) that was controlled by an Axon Instruments Digidata 1550 interface (Molecular Devices) and pClamp 10.4 software (Axon/Molecular Devices). Quantal mEPSCs in HCs were detected and analyzed using Minianalysis 6.0.7 (Synaptosoft, Inc., Decatur, GA). Horizontal cell mEPSCs were detected using an amplitude threshold of 1.5 pA and an area threshold of 1.5 fC. Rod and cone presynaptic events were detected using an amplitude threshold of 1.5 pA and an area threshold of 4.5 fC. Spontaneously occurring glutamate transporter currents in rods and cones showed slow kinetics, so detection parameters were adjusted to identify these events over a longer time period. After automated detection, each mEPSC was evaluated individually by eye and the peak amplitude recalculated as necessary. Double peaks were analyzed using an algorithm within Synaptosoft that adjusts the baseline of the second peak by extrapolating the exponential decay of the first peak. For the large number of records analyzed for bafilomycin experiments in Fig. 5, we used automated detection without manual correction and a threshold of 2 pA. This yielded qualitatively similar results as manually curated analysis but with lower frequencies due to an under-counting of closely spaced events.

Presynaptic currents in rod and cone photoreceptors arising from activation of glutamate transporter currents were measured using a pipette solution that contained 90 mM potassium thiocyanate in place of the 40 mM Cs glutamate and 50 mM Cs gluconate (Picaud et al., 1995; Szmajda & Devries, 2011). Use of thiocyanate enhanced the anion currents associated with glutamate transporter activation. Photoreceptors were voltage clamped at −70 mV. In some of these recordings, 10 mM BAPTA was also included in the pipette solution to buffer Ca^{2+}.

Imaging

For imaging experiments with TIRF microscopy, isolated rod photoreceptors were used. The retina was dissected under infrared illumination and isolated in a standard amphibian saline solution. The tissue was kept in darkness to maintain rods in a depolarized state and incubated with a 10-kDa dextran-conjugated, pH-sensitive form of rhodamine (pHrodo, 500 μg/ml; Invitrogen) for 3 min at 20°C. This brief incubation period loads a small fraction (~3%) of synaptic vesicles allowing individual vesicles to be visualized under TIRF illumination (Chen et al., 2013). After dye loading was complete, retinas were placed in a nominally Ca^{2+}-free saline solution and exposed to light to limit further vesicle cycling. The

nominally Ca^{2+}-free solution contained (in mM): 111 NaCl, 2.5 KCl, 5 $MgCl_2$, 5 glucose, and 10 HEPES (pH 7.8). Next, the retina was prepared for dissociation by incubation with papain (30 U/ml; Worthington) plus cysteine (0.2 mg/ml) in this Ca^{2+}-free solution for 35 min at 20°C. The tissue was then washed and triturated using a fire-polished Pasteur pipette. The cell suspension containing isolated rods was transferred onto 1.78 refractive index glass coverslips (Olympus) coated with Cell-Tak (3.5 μg/cm^2; BD Biosciences) 30 min prior to imaging. During TIRF imaging experiments, the tissue was maintained at room temperature in standard amphibian saline solution with the addition of Cd^{2+} (100 μM) to block Ca^{2+} channels plus dantrolene (10 μM) to block Ca^{2+}-induced Ca^{2+} release (CICR). Imaging was done using a 1.65 numerical aperture objective (Apo 100X oil; Olympus) and a 561 nm solid-state laser (Melles Griot) was used to illuminate pHrodo-loaded vesicles. With total internal reflection, the 561 nm evanescent field had a length constant of 60 nm (Chen et al., 2013). Fluorescence emission of pHrodo-loaded vesicles was collected through a 609 nm (54 nm wide) bandpass filter (Semrock) and imaged by an EMCCD camera at 40 ms/frame (Hamamatsu ImageEM) with a pixel size of 80 nm/pixel. Data were acquired and analyzed using MetaMorph software (Molecular Devices).

Imaging trials with pHrodo were conducted in isolated rods that were voltage clamped at −70 mV in the presence of Cd^{2+} plus dantrolene. In addition to the standard pipette solution, the patch pipette contained a RIBEYE-binding peptide with an N-terminal fluorophore, Hylite, (Hylite488-EQTVPVDLSVARPR, 80 μM) which allowed us to visualize synaptic ribbons. The peptide binds selectively to the ribbon protein, RIBEYE, through a PXDLS peptide sequence in the B domain of RIBEYE (Zenisek et al., 2004; Zenisek, 2008; Snellman et al., 2011). Fluorescently-labeled synaptic ribbons were visualized using 488-nm laser excitation and 525-nm emission. Ribbons are not located immediately adjacent to the rod membrane but sit atop the arciform density within invaginating ribbon synapses. To visualize HyLite488-labeled ribbons, we therefore elevated the incident angle of the 488 nm laser to allow light to penetrate the cell more deeply. We measured the distance between individual release events and the center of the nearest synaptic ribbon. In some instances, pHrodo-loaded vesicles approached the plasma membrane but were not released. Release events were distinguished from non-release departure events based on the more rapid decline in fluorescence following fusion and subsequent release of pHrodo. Release events were defined as a decline in peak fluorescence intensity exceeding 50% within the first frame and more than 80% within two 40-ms frames with a total decrease in fluorescence of >90% relative to baseline. These are more stringent criteria than used previously by Chen et al., 2013.

Pharmacology

Unless otherwise noted, drugs were dissolved in amphibian saline solution and superfused over the slice preparations. Cadmium ($CdCl_2$, 100–500 μM Sigma Chemicals) was used to block influx through Ca^{2+} channels. The ryanodine receptor blocker, dantrolene (10 μM), was used to block Ca^{2+} release from internal stores (Chen et al., 2014). Due to concerns about incomplete recovery after washout, each slice preparation was exposed to Cd^{2+} only once and then new slices were prepared for subsequent experiments. In some experiments,

retinal slices were incubated with 100 μM EGTA-AM (Life Technologies) for 2 hours to increase intracellular Ca^{2+} buffering prior to starting electrophysiological recordings

Analysis

Whole cell and paired recordings were analyzed with pClamp 10.4 software. Data were further analyzed and plotted with GraphPad Prism 4. Average values were reported as mean ± SEM unless otherwise noted. Statistical significance was evaluated using two-tailed independent or paired Student's t tests and Bonferroni's multiple comparison test with $p < 0.05$. A Kolmogorov–Smirnov test (KS test) was used to compare cumulative frequency curves.

Results

HC mEPSCs persist when synaptic Ca^{2+} is reduced

The persistence of mEPSCs in bipolar cells following application of 2 mM Co^{2+} in nominally Ca^{2+}-free solution suggests that there may be a mechanism for Ca^{2+}-independent release of vesicles from photoreceptors (Maple et al., 1994). However, the effects of nominally Ca^{2+}-free solutions on membrane surface charge can shift the activation of L-type Ca^{2+} currents to more negative potentials and thereby allow functionally significant currents to persist at the photoreceptor resting membrane potential even in the presence of Co^{2+} (Piccolino et al., 1996, 1999; Piccolino & Pignatelli, 1996). We therefore tested effects on HC mEPSCs of inhibiting Ca^{2+} channels with Cd^{2+} (100 μM) in which the blocking effect is due to pore block rather than surface charge effects as with Co^{2+} (Piccolino & Pignatelli, 1996). CICR is an important contributor to release from rods (Suryanarayanan & Slaughter, 2006; Babai et al., 2010; Chen et al., 2014) and so we also inhibited CICR with dantrolene (10 μM). In light-adapted retinas under control conditions, we consistently detected mEPSCs in HCs arising from spontaneous release events. HCs in salamander retina receive both rod and cone inputs (Thoreson et al., 2002; Zhang et al., 2006), so HC mEPSCs likely derived from both cell types. Fig. 1A shows a segment from a representative trace with multiple mEPSCs. Even in this light-adapted preparation, resting potentials of photoreceptors can be sufficiently depolarized to activate L-type Ca^{2+} channels in their synaptic terminals. If the spontaneous mEPSCs in control conditions were entirely due to Ca^{2+} entry and/or CICR, then application of Cd^{2+} plus dantrolene should completely abolish these events. Cd^{2+} (100 μM) blocks rod Ca^{2+} currents (N = 4 rods, data not shown) and dantrolene (10 μM) blocks CICR in rods (Chen et al., 2014). We found that, although the frequency diminished considerably, a number of mEPSCs persisted in Cd^{2+} plus dantrolene. This is illustrated by a representative trace from the same cell in Fig. 1B. Fig. 1C and D show mEPSC amplitude distributions from the same cell in control and Cd^{2+} plus dantrolene conditions. In control conditions, mEPSCs in this HC averaged 4.03 pA in amplitude. While smaller than mEPSCs found at many conventional synapses, they were similar in amplitude to mEPSCs reported previously in salamander and mammalian HCs (Maple et al., 1994; Cadetti et al., 2005; Devries et al., 2006; Feigenspan & Babai, 2015). Application of Cd^{2+} plus dantrolene slightly reduced the mean amplitude of mEPSCs to 3.33 pA (Fig. 1 B and D). Much, if not all, of this amplitude reduction appears to be due to under-counting of small events when

release frequency is high and the presence of more large, presumably multiquantal, events in control conditions.

To compare kinetics of mEPSCs in control vs. Cd^{2+} plus dantrolene conditions, we analyzed ~100 well-isolated events in both conditions to determine rise and decay time constants. In control, rise times averaged 1.72 ± 0.06 ms and decay times averaged 2.13 ± 0.13 ms. The rise and decay times in Cd^{2+} plus dantrolene did not differ significantly, averaging 1.73 ± 0.10 ms and 2.04 ± 0.29 ms respectively (rise P = 0.93, decay P = 0.75, unpaired t-tests).

We tested various blocking agents to examine sources of Ca^{2+} driving Ca^{2+}-dependent spontaneous release. In control conditions, the frequency ranged from 23 to 245 Hz, averaging 115.2 ± 10.1 Hz (N=28; median = 114 Hz). In Cd^{2+} plus dantrolene, the frequency averaged 38.5 ± 10.7 Hz (N = 11 HCs), ranging from 3 to 119 Hz with a median value of 27.4 Hz that was lower than the mean. Application of 100 μM Cd^{2+} alone reduced frequency by a similar amount (37.0 ± 12.4 Hz, N=8; median = 26.8 Hz). A higher concentration of Cd^{2+} (500 μM) caused a somewhat greater reduction (14.5 ± 2.7 Hz, N=8; median = 15.8 Hz). To test the possibility that spontaneous release might be mediated by Ca^{2+} influx through other types of Ca^{2+}-permeable channels that were not blocked by Cd^{2+}, we applied a Ca^{2+}-free solution plus EGTA (1 mM) to ensure removal of residual Ca^{2+} from the extracellular solution. With 0 Ca^{2+} extracellular solution, the frequency of mEPSCs was also reduced significantly relative to control (Fig. 2A, 24.5 ± 12.1 Hz, $P < 0.05$, N = 5 HCs, unpaired t-test), but was not significantly lower than Cd^{2+} plus dantrolene (P = 0.45, unpaired t-test). This suggests that influx through other Ca^{2+}-permeable channels did not contribute significantly to spontaneous release. Consistent with this, combining Cd^{2+} (100 μM) with Gd^{3+} (30 μM) to block Ca^{2+}-permeable store-operated channels also did not further reduce mEPSC frequency (40.5 ± 9.4 Hz, P = 0.90, N = 7 HCs).

The amplitude of Ca^{2+}-independent spontaneous release events in 100 μM Cd^{2+} (4.0 ± 0.37 pA, N=8), 100 μM Cd^{2+} plus dantrolene (3.9 ± 0.68 pA, N=11), 500 μM Cd^{2+} (3.8 ± 0.35 pA, N=8), 100 μM Cd^{2+} plus 30 μM Gd^{3+} (3.8 ± 0.27 pA, N=7), and 0 Ca^{2+} plus 1 mM EGTA (3.2 ± 0.33 pA, N=5) conditions were smaller than control mEPSC amplitudes (4.8 ± 0.34 pA, N=28) but these differences did not attain statistical significance. As mentioned above, these smaller amplitudes were at least partly due to difficulties in detecting small events when release occurred at high frequency and a higher frequency of large, presumably multiquantal, events in control conditions.

The residual release seen in conditions where Ca^{2+} influx was blocked shows that there is a component of spontaneous vesicle release from photoreceptors that does not require Ca^{2+} influx through membrane channels. Photoreceptor synapses employ an exocytotic Ca^{2+} sensor with an unusually low Ca^{2+} threshold of only ~400 nM (Thoreson et al., 2004; Duncan et al., 2010). We therefore tested whether basal levels of intracellular Ca^{2+} may be sufficient to drive vesicle release. After incubating retinas in EGTA-AM (100 μM) for 2 hours, the frequency of mEPSCs was reduced significantly (Fig. 2A, 67.2 ± 16.0 Hz, $P < 0.05$, N = 10 HCs, unpaired t-test). The addition of Cd^{2+} plus dantrolene to slices incubated in EGTA-AM reduced mEPSC frequency to levels similar to those observed after application of Cd^{2+} plus dantrolene in untreated slices (Fig. 2A, 35.3 ± 12.0 Hz, N = 9 HCs).

Nanodomains of Ca^{2+} were unlikely to be responsible for the remaining release, since these should be abolished by blockade of Ca^{2+} channels with Cd^{2+}.

Another possible mechanism by which extracellular Ca^{2+} has been shown to trigger spontaneous release is by activation of Ca^{2+}-sensing receptors (Vyleta & Smith, 2011). We tested a positive allosteric modulator for Ca^{2+}-sensing receptors, calindol (5 μM) and observed no significant effect on mEPSC frequency (KS test, P = 0.81, N = 6) or amplitude (Kolmogorov Smirnov test, P = 0.70, N = 6). Furthermore, such a mechanism cannot explain the persistence of mEPSCs in 0 Ca^{2+} extracellular solution.

mEPSCs result from glutamate release by rods and cones

In addition to producing post-synaptic currents in HCs, the release of glutamate-filled vesicles from photoreceptors activates glutamate transporters on their presynaptic terminals (Picaud et al., 1995; Grant and Werblin, 1996). Activation of glutamate transporters generates anion currents that can be used to detect release events presynaptically. To enhance glutamate transporter anion currents, we recorded from rods and cones using a patch pipette solution containing thiocyanate as the primary anion (Szmajda & Devries, 2011). In rods voltage clamped at −70 mV with this pipette solution, we observed spontaneous, transient inward currents (Fig. 3). Consistent with earlier studies on transporter anion currents in salamander photoreceptors (Grant and Werblin, 1996), presynaptic events were blocked by a glutamate transport inhibitor, TBOA (100 μM; N = 4; Fig. 3A). Application of Cd^{2+} (100 μM; Fig. 3B) significantly reduced the frequency of rod presynaptic events relative to control conditions (14.8 ± 1.2 Hz control, N = 23; 9.4 ± 1.4 Hz Cd^{2+}, N = 13; unpaired t-test, P = 0.009; paired t-test P = 0.0012, N = 6 rods). Fewer large events were observed in Cd^{2+} (Fig. 3C), but the overall mean amplitude of rod presynaptic events was not reduced significantly (Fig. 3D, 6.4 ± 0.6 pA control, N = 23; 5.9 ± 1.5 pA Cd^{2+}, N = 13; unpaired t-test, P = 0.58; paired t-test P = 0.30, N = 6 rods). The frequency of presynaptic events was also reduced significantly by including 10 mM BAPTA in the patch pipette solution to buffer intracellular Ca^{2+} (Fig. 3D; 5.9 ± 1.5 Hz, N = 9, P=0.003, unpaired t-test). Event amplitude was not significantly altered (4.8 ± 0.4 pA, P=0.39, unpaired t-test). As illustrated by the average event waveforms (Fig. 3E), rise and decay times were slightly faster in Cd^{2+} (10–90% rise time: control, 4.00 ± 0.47 ms; Cd^{2+}, 2.57 ± 0.36 ms; P = 0.0435. Decay time: control, 4.59 ± 0.49 ms, Cd^{2+}, 2.79 ± 0.35 ms, P = 0.0148). Large events showed slower kinetics than small events in rods and so this difference was at least partly due to the occurrence of fewer large events in Cd^{2+}. The reduction in event frequency produced by Cd^{2+} indicates that some of the spontaneous release events in rods that were voltage-clamped at −70 mV were Ca^{2+}-dependent events triggered by occasional openings of Ca^{2+} channels that can occur even at this very negative membrane potential. The events that remained after blocking Ca^{2+} channels with Cd^{2+} were due to Ca^{2+}-independent release. Cd^{2+} caused a greater reduction in the frequency of HC mEPSCs because, unlike measurements of rod transporter currents, photoreceptors were not voltage-clamped in those earlier experiments, allowing for a greater frequency of presynaptic Ca^{2+} channel openings.

These presynaptic recordings showed that Ca^{2+}-independent events can originate from rods. In salamander retina, HCs receive mixed inputs from both rods and cones (Zhang et al.,

2006), so we used presynaptic recordings to test whether cones were also capable of Ca^{2+}-independent vesicle release. As with rods, we observed quantal presynaptic glutamate transporter anion currents in cones voltage-clamped at −70 mV under control conditions and these presynaptic events were abolished by TBOA (100 μM; N = 6; Fig. 4A). Application of Cd^{2+} (100 μM) blocked cone Ca^{2+} currents (N = 6 cones) but presynaptic quantal events persisted (Fig. 4B). Unlike rods, the average frequency of presynaptic events in cones was not reduced significantly by application of Cd^{2+} (Fig. 4D; 12.6 ± 0.77 Hz control; 10.4 ± 1.6 Hz Cd^{2+}; paired t-test P = 0.35, N = 6 cones). There was also not a significant change in the amplitude of cone presynaptic events (Fig. 4C-D; 6.96 ± 0.54 pA control; 7.57 ± 1.38 pA Cd^{2+}; paired t-test P = 0.69, N = 6 cones). Introducing 10 mM BAPTA into cones through the patch pipette also did not significantly reduce event frequency (14.4 ± 1.51 Hz, N=7, unpaired t-test, P=0.32) or amplitude (8.03 ± 1.01 pA, P=0.39, unpaired t-test, Fig. 4D). These data suggest that most of the spontaneous release events observed in cones voltage-clamped at −70 mV are Ca^{2+}-independent. The kinetics of presynaptic events in cones were slower than those in rods (10–90% rise time, 8.25 ± 0.26 ms; decay time, 12.1 ± 1.23 ms, N = 6 cones; Fig. 4E), which may reflect rod-cone differences in the locations of glutamate transporters relative to release sites (Vandenbranden et al., 2000; Hasegawa et al., 2006; Rowan et al., 2010). Event kinetics in cones did not change significantly in Cd^{2+} (Cd^{2+}: 10–90% rise time, 7.94 ± 0.61 ms, P = 0.37, paired t-test; decay time, 10.8 ± 1.53 ms, P = 0.68; Fig. 4E).

Independence of vesicle pools involved in spontaneous and evoked release

There is evidence at some synapses that spontaneous release may involve different pools of synaptic vesicles than evoked release (Kaeser & Regehr, 2014; Kavalali, 2015; Schneggenburger & Rosenmund, 2015). To examine this question, we used an approach similar to Sara et al. (2005) and inhibited vesicular ATPase activity with bafilomycin, which in turn inhibits glutamate refilling of vesicles. We compared the rates of decline in evoked EPSCs and spontaneous mEPSCs during bafilomycin application. To evoke EPSCs, we obtained paired whole cell recordings from a rod and post-synaptic HC and then stimulated the rod with a depolarizing voltage step (−70 to −10 mV, 100 ms) at one-minute intervals. As illustrated in Fig. 5A and B, a depolarizing voltage step applied to rods typically evokes an initial fast EPSC followed by slower EPSC components. The initial fast component has been shown to be due to release from synaptic ribbons (Chen et al., 2013, 2014). The second slower component is primarily due to non-ribbon release driven by CICR (Chen et al, 2014). Slow EPSC components can also arise from release by neighboring rods stimulated by the flow of depolarizing current through gap junctions (Cadetti et al., 2006; Chen et al., 2014). We reduced release from neighboring coupled rods by hyperpolarizing them with use of a bright background light (Chen et al., 2014; Van Hook & Thoreson, 2015). Figs. 5C and D plot the amplitude of the fast, ribbon-mediated component (C) and the second, slower, non-ribbon component (D) as a function of time. In control conditions, EPSCs exhibited rundown during paired recording, with the faster ribbon-mediated EPSC component showing more rapid rundown than the slower component. Applying bafilomycin (7 μM) slightly accelerated the decline in both fast and slow EPSC components (comparing the change in normalized EPSC amplitude of the first 3 vs. last 3 responses from rod/HC pairs in control N=9 vs. bafilomycin N=8: peak 1, P = 0.65; peak 2, P=0.44, unpaired t-tests). HC

mEPSCs were collected in 10 s trials while the rod was voltage clamped at −70 mV. EPSC and mEPSC trials alternated every 30 s. Bafilomycin caused a significantly more rapid decline in both frequency (Fig. 5E) and amplitude (Fig. 5F) of spontaneous mEPSCs (comparing the normalized frequency and amplitude from the first 3 vs. last 3 records in control vs. bafilomycin: frequency $P < 0.04$, amplitude $P < 0.04$, $N = 7$ HCs bafilomycin, $N = 8$ HCs control, unpaired t-test). The decline in mEPSC amplitude involves incomplete re-filling of vesicles following their turnover (Cavelier & Attwell, 2007), which might also contribute to a decrease in release probability (Rost et al., 2015). If the pools involved in spontaneous and evoked release mixed thoroughly, then one would predict that treatment with bafilomycin should produce an equally rapid decline in both EPSCs and mEPSCs. The finding that the amplitude and frequency of spontaneous mEPSCs were reduced more rapidly than evoked EPSCs is thus consistent with the suggestion that vesicle pools involved in spontaneous and evoked release may be partially distinct from one another.

Spontaneous release can occur at ribbon and non-ribbon sites

Evoked release appears to occur only at ribbons in cones (Snellman et al., 2011; Van Hook & Thoreson, 2015) and so the persistence of spontaneous events in cones following application of Cd^{2+} suggests that Ca^{2+}-independent release can occur at ribbons. In rods, evoked release can occur at both ribbon and non-ribbon sites (Chen et al., 2013; Zampighi et al. 2011). In rods, but not cones, Ca^{2+} channel openings can trigger non-ribbon release by activating Ca^{2+}-induced Ca^{2+} release (CICR) (Križaj et al., 1999; Cadetti et al., 2006; Suryanarayanan & Slaughter, 2006; Babai et al., 2010; Chen et al., 2014). We visualized sites of Ca^{2+}-independent release in isolated rods using TIRF microscopy as described by Chen et al. (2013). After enzymatic isolation of individual rods, the synaptic terminal at the end of a thin axon settled and sometimes adhered to the glass coverslip, making it amenable for TIRF. We did not study cones because their synapses are located at the base of the cell body and rarely adhered to the coverslip as needed for TIRF. To visualize individual release events, vesicles within rod terminals were loaded with a 10-kD dextran-conjugated pH-sensitive form of rhodamine (pHrodo). This dye fluoresces in the acidic conditions within a vesicle, but its fluorescence is quickly quenched when exposed to the slightly alkaline extracellular medium. We incubated dark-adapted retinas for 3 minutes with the dye to load approximately 3% of the vesicles in a rod, allowing us to visualize individual vesicle fusion events (Chen et al., 2013). We measured Ca^{2+}-independent spontaneous release events in voltage-clamped rods (−70 mV) in the presence of Cd^{2+} (100 μM) plus dantrolene (10 μM) to block influx through Ca^{2+} channels and efflux from internal stores. To identify ribbon locations, we introduced a ribbon-targeted peptide (80 μM) conjugated to the fluorophore, HiLyte488, through a patch pipette. The evanescent field used for imaging of pHrodo-filled vesicles had a length constant of 60 nm. However, ribbons sit atop the arciform density within the invaginating synapse and were thus often not visible within this narrow evanescent field (Chen et al., 2013). To visualize HyLite488-labeled ribbons, we therefore elevated the incident angle of the 488 nm laser to allow light to penetrate the cell more deeply. As a rule, fluorescently-labeled ribbons were located deeper in the cell than sites of release visualized using pHrodo fluorescence, consistent with release occurring at the base of the ribbon (Vaithianathanet al., 2016). Synaptic terminals flatten out on the glass and so some of the ribbons that we observed may have faced upwards away from the membrane on

the glass. In Fig. 6A, one can see the faint fluorescent footprint of a rod terminal membrane pressed against the coverslip. Part of the axon and soma are also visible. Two fluorescently-labeled ribbons appear as adjacent bright spots in the upper right of the terminal. Small white circles mark the locations of individual Ca^{2+}-independent spontaneous vesicle release events observed in the presence of Cd^{2+} plus dantrolene. A few of these events occurred beneath the ribbons but others occurred some distance away (Fig. 6A).

We observed 66 release events in 9 rod terminals. These events were acquired from a total of 106 trials (6–18 trials/cell) at 400 frames/trial and 40 ms/frame. Assuming 3% of vesicles were loaded with dye, this suggests an observed release frequency in Cd^{2+} and dantrolene of 1.3 Hz. Only a portion of the terminal membrane area is attached to the glass and thus visible by TIRF microscopy, so the total release rate in each terminal would be more than twice as great, in rough agreement with electrophysiological rate measurements made from individual rods which have an average of 1.6 terminals apiece (Thoreson and Van Hook, 2015). We plotted the distance from each individual release event to the nearest ribbon (Fig. 6B). The distance from a release event to the center of its nearest neighbor ribbon averaged 1.80 ± 0.14 μm (N = 66 events in 9 rods). The length of HiLyte488-labeled ribbons along the X-Y plane averaged 0.47 ± 0.06 μm (N = 28 ribbons). The maximum possible distance between release events and the nearest ribbon is limited by the size of the synaptic terminal footprint on the glass. We found that more than 60% of release events occurred at locations more than 1 μm away from the nearest synaptic ribbon. By comparison, >80% of release events evoked by a strong depolarizing step occurred within 1 μm of ribbons (Chen et al., 2013). More distant annular rings have larger surface areas for fusion and so we converted distance measurements into radial density distributions. The highest density of release events occurred 1–1.4 μm from a ribbon (Fig. 6B). These data indicate that Ca^{2+}-independent spontaneous release can occur at both ribbon and non-ribbon sites in rods and that non-ribbon sites appear to be responsible for a large fraction of spontaneous release events.

Discussion

Mechanisms of Spontaneous Release

There is evidence for both Ca^{2+}-dependent and Ca^{2+}-independent components to spontaneous release in various neurons (Kaeser & Regehr, 2014; Kavalali, 2015; Schneggenburger & Rosenmund, 2015). A number of studies have found that spontaneous release depends upon intracellular Ca^{2+}, although the sources of Ca^{2+} can vary. Ca^{2+} entry through a variety of Ca^{2+}-permeable ion channels can contribute to spontaneous release. Spontaneous release can be reduced substantially by introducing the Ca^{2+} chelators BAPTA or EGTA into neurons (Xu et al., 2009; Goswami et al., 2012; Ermolyuk et al., 2013; Schneider et al., 2015). Antagonism of voltage-gated Ca^{2+} channels in cortical and cerebellar neurons reduced spontaneous release by about 50% (Goswami et al., 2012; Williams et al., 2012). In brainstem neurons, Ca^{2+} influx through tonically active TRPV1 receptors accounted for a substantial fraction of spontaneous release (Shoudai et al., 2010; Peters et al., 2010). Activation of Ca^{2+}-permeable P2X2 receptors (Khakh, 2009) and release of intracellular Ca^{2+} from internal stores can also trigger spontaneous mEPSCs (Emptage et al., 2001; Xu et al., 2009). However, other studies have found that spontaneous release does

not always require elevation of intracellular [Ca^{2+}]. For example, blocking voltage-gated Ca^{2+} channels did not alter spontaneous release in CA3 neurons (Scanziani et al., 1992). In neocortical neurons, spontaneous release was found to depend on Ca^{2+}-sensing G protein-coupled receptors that are activated by extracellular rather than intracellular Ca^{2+} (Vyleta & Smith, 2011).

Vertebrate photoreceptors do not exhibit fast sodium-dependent action potentials but instead vary their membrane potential continuously with changes in light intensity and the state of adaptation. The resting membrane potential of rods and cones is near −40 mV in darkness, stimulating the opening of Ca^{2+} channels and driving continuous release of vesicles. As expected, we found that inhibiting Ca^{2+} influx caused a decrease in mEPSC frequency. However, it did not eliminate release. We observed spontaneous quantal glutamate transporter currents in rods and cones that were voltage clamped at −70 mV, where L-type Ca^{2+} channels generally remain in the closed state. In rods, these currents were further reduced in frequency, but not eliminated, by blocking Ca^{2+} channels with Cd^{2+}. These data suggest that there are three forms of basal release from photoreceptors: 1) Ca^{2+}-dependent, evoked release driven by the voltage-dependent activation of L-type Ca^{2+} channels, 2) Ca^{2+}-dependent spontaneous release that can occur in rods even when they are hyperpolarized to a potential where Ca^{2+} channels are normally closed, and 3) Ca^{2+}-independent spontaneous release that persists after inhibiting Ca^{2+} influx with Cd^{2+} or Ca^{2+}-free extracellular solutions. The mEPSCs that remain after blocking influx of Ca^{2+} are due to a Ca^{2+}-independent release mechanism that does not require Ca^{2+} influx, Ca^{2+} release from intracellular stores, or high basal levels of intracellular Ca^{2+}.

Some studies suggest that different molecular mechanisms mediate evoked and spontaneous release, whereas others suggest that the same mechanisms may mediate both (Deitcher et al., 1998; Deak et al., 2006; Glitsch, 2008; Smith et al., 2012; Kaeser & Regehr, 2014). The original hypothesis to explain the origins of spontaneous release was that it might occur through SNARE-mediated membrane fusion driven by Ca^{2+}-independent, thermodynamic changes in SNARE conformation. But it has also been proposed that a special Ca^{2+} sensor such as Doc2 may mediate Ca^{2+}-dependent spontaneous release (Groffen et al., 2010). Doc2 might also be involved in Ca^{2+}-independent spontaneous release (Pang et al., 2011). Although its molecular identity remains unclear, the sensor that mediates exocytosis at photoreceptor synapses shows an unusually high Ca^{2+} affinity and low cooperativity (Thoreson et al., 2004; Duncan et al., 2010), properties that are similar to the sensor thought to mediate asynchronous and spontaneous release at other synapses (Lou et al., 2005; Sun et al., 2007). It has also been suggested that distinct SNARE proteins, such as the non-canonical SNAREs VAMP7 (Hua et al., 2011) and Vti1a (Ramirez et al., 2012) may mediate spontaneous release (Hua et al., 1998; Scheuber et al., 2006). Differences in SNARE configurations caused by different SNARE isoforms or associated proteins might alter the preference for spontaneous or evoked release (Maximov et al., 2009; Buhl et al., 2013) by altering the domain structure of the SNARE complex (Weber et al., 2010). For example, the expression of complexin 3/4 subtypes at ribbon synapses constrains ongoing spontaneous release from bipolar cells (Vaithianathan et al., 2013, 2015). Thus, while multiple molecular mediators for spontaneous release have been proposed, a definitive mechanism is not currently known.

Characteristics of Ca^{2+}-independent Spontaneous Release

Evoked and spontaneous release can occur at distinct sites. Imaging of release events at individual *Drosophila* neuromuscular junctions showed that evoked and spontaneous release can occur at spatially distinct synapses (Melom et al., 2013; Peled et al., 2014). In hippocampal neurons, different populations of NMDA receptors respond to evoked and spontaneous release (Atasoy et al., 2008) suggesting spatial separation of the two forms of release. TIRF imaging studies of single vesicle release at retinal bipolar cell synapses showed that evoked release events clustered near ribbons whereas spontaneous release events often occurred at non-ribbon sites (Zenisek, 2008). Our TIRF results showed that when Ca^{2+} channels were blocked with Cd^{2+}, release from rods occurred at sites both near and far from ribbons although the density of release events rose closer to ribbons. The relative frequency of non-ribbon release was higher for Ca^{2+}-independent spontaneous release than was previously found for evoked release (Chen et al., 2013). Spontaneous release in the absence of Cd^{2+} involves both Ca^{2+}-independent release as well as release triggered by occasional Ca^{2+} channel openings. Because Ca^{2+} channels are clustered near ribbons (Nachman-Clewner et al., 1999; Morgans, 2001), spontaneous release under such conditions would thus be expected to involve more ribbon-related release events than purely Ca^{2+}-independent release. Post-synaptic recordings from HCs that receive both rod and cone inputs and presynaptic recordings from individual rods and cones showed that Ca^{2+}-independent spontaneous release can occur in both rods and cones. In cones, evoked release occurs only at ribbons so perhaps spontaneous release in these cells also occurs only at ribbons (Snellman et al., 2011; Van Hook & Thoreson, 2015). Consistent with this possibility, evoked release from rod bipolar cells also occurs mostly at ribbons (Snellman et al., 2011) and the frequency and amplitude of spontaneous mEPSCs evoked by bipolar cell release were decreased following ribbon damage (Mehta et al., 2013). On the other hand, a recent study found that spontaneous release from rod bipolar cells was not diminished by the loss of ribbons in RIBEYE knockout mice (Maxeiner et al., 2016). Glutamate transporters are located perisynaptically in rods (Hasegawa et al., 2006) and so a relative increase in the likelihood of non-ribbon release events during Ca^{2+}-independent release might contribute to faster kinetics of presynaptic transporter currents in rods in these conditions. We did not observe significant changes in the kinetics of HC mEPSCs after blocking Ca^{2+} entry. Simulations of rod synapses indicate that glutamate can rise quickly within the entire invaginating ribbon synapse, attaining levels above the EC50 for glutamate on horizontal cells at distances quite far from release sites (32 μM; Gaal et al., 1998; Rao-Mirotznik et al., 1998). This may limit the impact of differences in release site location on the kinetics of HC mEPSCs. The affinity of glutamate exhibited by heterologously expressed AMPA receptors has been found to range from 1–560 μM (Traynelis et al., 2010). If receptors are less sensitive to glutamate, then the likelihood that rare spontaneous events occurring at distant ectopic sites will have a significant impact on HC membrane potential diminishes. Conversely, if receptors are more sensitive, the likelihood of significant impact increases.

The question of whether spontaneously released vesicles derive from the same pool as evoked release has received much attention with evidence for both pool separation (Sara et al., 2005; Fredj & Burrone, 2009) and pool mixing (Groemer & Klingauf, 2007; Hua et al., 2010). Unlike conventional synapses where few vesicles are mobile, 85% of the cytoplasmic

vesicles in cone and bipolar ribbon synapses are mobile (Rea et al., 2004; Holt et al., 2004). It has been suggested that spontaneous release may originate from a pool of less mobile vesicles (Fredj & Burrone, 2009) and/or be segregated into evoked and spontaneous pools by molecular markers (Hua et al., 2011; Ramirez et al., 2012). Vesicle pool separation would limit the ability of ongoing spontaneous release to deplete releasable vesicles from the evoked pool. We found that bafilomycin caused a more rapid decline in spontaneous mEPSCs--consisting of a mixture of both Ca^{2+}-dependent and Ca^{2+}-independent release--than in evoked EPSCs. This is consistent with the idea that vesicles involved in evoked and at least one form of spontaneous release may originate from different vesicle pools. However, there are also other possible explanations for these results. For example, it may be that partially filled vesicles can be released spontaneously but that evoked release shows a preference for fully filled vesicles (Rost et al. 2015). Another possibility is that if spontaneous release occurs more frequently at distant sites than evoked release, then effects of bafilomycin might have a stronger effect on spontaneous events due to a lower glutamate concentration at post-synaptic receptors. Reduced vesicle filling would affect events generated by low glutamate levels more strongly than events generated by higher glutamate levels.

Functional Impact of Spontaneous Release

A number of functions for spontaneous release have been proposed, including maintenance of synaptic connections and potentiation of post-synaptic receptors (McKinneyel al., 1999; Kombian et al., 2000; Carter & Regehr, 2002; Sutton et al., 2006). Photoreceptor synapses do not show any evidence for synaptic potentiation. The frequency of Ca^{2+}-dependent release events in rods, even when they are hyperpolarized to −70 mV, would seem sufficient for post-synaptic cells to recognize that connections are still present. In cones, the frequency of release events did not diminish after blocking Ca^{2+} entry so Ca^{2+}-independent release may be more important for maintaining connectivity at cone synapses.

While its functional significance is not entirely clear, one functional consequence of Ca^{2+}-independent spontaneous release at photoreceptor synapses would be to increase noise. Ca^{2+}-independent spontaneous mEPSCs in HCs showed an average frequency of 14 Hz in the presence of 500 μM Cd^{2+}, but the rate of release at any individual presynaptic release site is far lower. Lasansky (1978) reported that each OFF-bipolar cell in salamander retina received 30–50 contacts from 10–15 photoreceptors. Horizontal cells have larger light responses and larger dendritic fields than OFF-bipolar cells, so HCs are likely to receive more photoreceptor contacts than OFF-bipolar cells. In cones, there appear to be ~15–20 vesicle release sites at the base of each ribbon (Bartoletti et al., 2010; Thoreson et al., 2016). In rods, the readily releasable pool averages ~24 vesicles/ribbon (Van Hook & Thoreson, 2015). If we assume that each HC receives at least 50 ribbon contacts and that each ribbon has ~20 release sites at its base, then input into a horizontal cell may arise from at least 1000 separate release sites. Given a post-synaptic frequency of 14 Hz for Ca^{2+}-independent spontaneous release, this suggests a frequency at each release site of < 0.015 Hz. Presynaptic recordings of glutamate transporter currents suggested a frequency of spontaneous Ca^{2+}-independent release of 6 Hz in single rods and 10 Hz in cones. If we assume that release occurs only at ribbons, then for rods and cones that have 7 and 13 ribbons per cell,

respectively (Bartoletti et al., 2011; Van Hook and Thoreson, 2015), this suggests a frequency of ~0.04 Hz/release site. Much of the Ca^{2+}-independent spontaneous release from rods occurs at non-ribbon sites, suggesting that the actual frequency at individual release sites in rods is even lower. These estimates approach the frequency of ~0.01 Hz observed at hippocampal synapses (Murthy & Stevens, 1999; Rhee et al., 2005; Arancillo et al., 2013) but are much higher than the frequency of ~0.002 Hz seen at the calyx of Held (Schneggenburger & Rosenmund, 2015). Our predicted rates are also consistent with the spontaneous fusion frequency of 0.02 Hz observed with *in vitro* fusion assays between vesicles expressing SNARE proteins plus synaptotagmin 1 and complexin 1 (Lai et al., 2014). The low frequency of spontaneous release in photoreceptors limits its impact on synaptic noise. Whether Ca^{2+}-independent spontaneous release is simply an unavoidable consequence of a fusion apparatus poised for release by low Ca^{2+} concentrations (Thoreson et al., 2004) or whether it may play a beneficial role in photoreceptors remains unclear.

Acknowledgments

This research is supported by the National Institutes of Health grants EY010542 (WT) and F32EY023864 (MJVH), a Senior Scientific Investigator Award from Research to Prevent Blindness (WT), and a Graduate Fellowship from UNMC (KC). Thanks to Dr. Minghui Chen for assistance with TIRF microscopy experiments and to Dr. David Zenisek for generously providing the RIBEYE-binding peptide.

Abbreviations

CICR	Ca^{2+}-induced Ca^{2+} release
HCs	horizontal cells
EPSCs	excitatory post-synaptic currents
mEPSCs	miniature excitatory post-synaptic currents
TIRF	total internal reflectance fluorescence

References

Arancillo M, Min SW, Gerber S, Münster-Wandowski A, Wu YJ, Herman M, Trimbuch T, Rah JC, Ahnert-Hilger G, Riedel D, Südhof TC, Rosenmund C. Titration of Syntaxin1 in mammalian synapses reveals multiple roles in vesicle docking, priming, and release probability. The Journal of Neuroscience. 2013; 33(42):16698–16714. [PubMed: 24133272]

Atasoy D, Ertunc M, Moulder KL, Blackwell J, Chung C, Su J, Kavalali ET. Spontaneous and evoked glutamate release activates two populations of NMDA receptors with limited overlap. The Journal of Neuroscience. 2008; 28(40):10151–10166. [PubMed: 18829973]

Babai N, Morgans CW, Thoreson WB. Calcium-induced calcium release contributes to synaptic release from mouse rod photoreceptors. Neuroscience. 2010; 165(4):1447–1456. [PubMed: 19932743]

Bartoletti TM, Babai N, Thoreson WB. Vesicle pool size at the salamander cone ribbon synapse. Journal of Neurophysiology. 2010; 103(1):419–423. [PubMed: 19923246]

Bartoletti TM, Jackman SL, Babai N, Mercer AJ, Kramer RH, Thoreson WB. Release from the cone ribbon synapse under bright light conditions can be controlled by the opening of only a few Ca(2+) channels. Journal of Neurophysiology. 2011; 106(6):2922–2935. [PubMed: 21880934]

Buhl LK, Jorquera RA, Akbergenova Y, Huntwork-Rodriguez S, Volfson D, Littleton JT. Differential regulation of evoked and spontaneous neurotransmitter release by C-terminal modifications of complexin. Molecular and Cellular Neuroscience. 2013; 52:161–172. [PubMed: 23159779]

Cadetti L, Tranchina D, Thoreson WB. A comparison of release kinetics and glutamate receptor properties in shaping rod-cone differences in EPSC kinetics in the salamander retina. Journal of Physiology. 2005; 569(Pt 3):773–788. [PubMed: 16223761]

Cadetti L, Bryson EJ, Ciccone CA, Rabl K, Thoreson WB. Calcium-induced calcium release in rod photoreceptor terminals boosts synaptic transmission during maintained depolarization. European Journal of Neuroscience. 2006; 23(11):2983–2990. [PubMed: 16819987]

Carter AG, Regehr WG. Quantal events shape cerebellar interneuron firing. Nature Neuroscience. 2002; 5(12):1309–1318. [PubMed: 12411959]

Cavelier P, Attwell D. Neurotransmitter depletion by bafilomycin is promoted by vesicle turnover. Neuroscience Letters. 2007; 412(2):95–100. [PubMed: 17123716]

Chen M, Križaj D, Thoreson WB. Intracellular calcium stores drive slow non-ribbon vesicle release from rod photoreceptors. Frontiers in Cellular Neuroscience. 2014; 8:20. [PubMed: 24550779]

Chen M, Van Hook MJ, Zenisek D, Thoreson WB. Properties of ribbon and non-ribbon release from rod photoreceptors revealed by visualizing individual synaptic vesicles. The Journal of Neuroscience. 2013; 33(5):2071–2086. [PubMed: 23365244]

Deak F, Shin OH, Kavalali ET, Sudhof TC. Structural determinants of synaptobrevin 2 function in synaptic vesicle fusion. The Journal of Neuroscience. 2006; 26:6668–6676. [PubMed: 16793874]

Deitcher DL, Ueda A, Stewart BA, Burgess RW, Kidokoro Y, Schwarz TL. Distinct requirements for evoked and spontaneous release of neurotransmitter are revealed by mutations in the Drosophila gene neuronal-synaptobrevin. The Journal of Neuroscience. 1998; 18(6):2028–2039. [PubMed: 9482790]

DeVries SH, Li W, Saszik S. Parallel processing in two transmitter microenvironments at the cone photoreceptor synapse. Neuron. 2006; 50(5):735–748. [PubMed: 16731512]

Duncan G, Rabl K, Gemp I, Heidelberger R, Thoreson WB. Quantitative analysis of synaptic release at the photo receptor synapse. Biophysical Journal. 2010; 98(10):2102–2110. [PubMed: 20483317]

Emptage NJ, Reid CA, Fine A. Calcium stores in hippocampal synaptic boutons mediate short-term plasticity, store-operated Ca^{2+} entry, and spontaneous transmitter release. Neuron. 2001; 29(1): 197–208. [PubMed: 11182091]

Ermolyuk YS, Alder FG, Surges R, Pavlov IY, Timofeeva Y, Kullmann DM, Volynski KE. Differential triggering of spontaneous glutamate release by P/Q-, N- and R-type Ca^{2+} channels. Nature Neuroscience. 2013; 16(12):1754–1763. [PubMed: 24185424]

Feigenspan A, Babai N. Functional properties of spontaneous excitatory currents and encoding of light/dark transitions in horizontal cells of the mouse retina. European Journal of Neuroscience. 2015; 42(9):2615–2632. [PubMed: 26173960]

Fredj NB, Burrone J. A resting pool of vesicles is responsible for spontaneous vesicle fusion at the synapse. Nature Neuroscience. 2009; 12(6):751–758. [PubMed: 19430474]

Gaal L, Roska B, Picaud SA, Wu SM, Marc R, Werblin FS. Postsynaptic response kinetics are controlled by a glutamate transporter at cone photoreceptors. Journal of Neurophysiology. 1998; 79(1):190–196. [PubMed: 9425190]

Glitsch MD. Spontaneous neurotransmitter release and Ca^{2+}--how spontaneous is spontaneous neurotransmitter release? Cell Calcium. 2008; 43(1):9–15. [PubMed: 17382386]

Goswami SP, Bucurenciu I, Jonas P. Miniature IPSCs in hippocampal granule cells are triggered by voltage-gated Ca^{2+} channels via microdomain coupling. The Journal of Neuroscience. 2012; 32:14294–14304. [PubMed: 23055500]

Grant GB, Werblin FS. A glutamate-elicited chloride current with transporter-like properties in rod photoreceptors of the tiger salamander. Visual Neuroscience. 1996; 13(1):135–144. [PubMed: 8730995]

Groemer TW, Klingauf J. Synaptic vesicles recycling spontaneously and during activity belong to the same vesicle pool. Nature Neuroscience. 2007; 10(2):145–147. [PubMed: 17220885]

Groffen AJ, Martens S, Díez Arazola R, Cornelisse LN, Lozovaya N, de Jong AP, Goriounova NA, Habets RL, Takai Y, Borst JG, Brose N, McMahon HT, Verhage M. Doc2b is a high-affinity Ca^{2+}

sensor for spontaneous neurotransmitter release. Science. 2010; 327(5973):1614–1618. [PubMed: 20150444]

Hasegawa J, Obara T, Tanaka K, Tachibana M. High-density presynaptic transporters are required for glutamate removal from the first visual synapse. Neuron. 2006; 50(1):63–74. [PubMed: 16600856]

Hirasawa H, Shiells RA, Yamada M. Analysis of spontaneous EPSCs in retinal horizontal cells of the carp. Neuroscience Research. 2001; 40(1):75–86. [PubMed: 11311408]

Holt M, Cooke A, Neef A, Lagnado L. High mobility of vesicles supports continuous exocytosis at a ribbon synapse. Current Biology. 2004; 14(3):173–183. [PubMed: 14761649]

Hua SY, Raciborska DA, Trimble WS, Charlton MP. Different VAMP/synaptobrevin complexes for spontaneous and evoked transmitter release at the crayfish neuromuscular junction. Journal of Neurophysiology. 1998; 80(6):3233–3246. [PubMed: 9862918]

Hua Y, Sinha R, Martineau M, Kahms M, Klingauf J. A common origin of synaptic vesicles undergoing evoked and spontaneous fusion. Nature Neuroscience. 2010; 13(12):1451–1453. [PubMed: 21102448]

Hua Z, Leal-Ortiz S, Foss SM, Waites CL, Garner CC, et al. v-SNARE composition distinguishes synaptic vesicle pools. Neuron. 2011; 71:474–487. [PubMed: 21835344]

Kaeser PS, Regehr WG. Molecular mechanisms for synchronous, asynchronous, and spontaneous neurotransmitter release. Annual Review of Physiology. 2014; 76:333–363.

Katz, B. The Sherrington Lectures. Springfield, IL: Thomas; 1969. The Release of Neural Transmitter Substances.

Kavalali ET. The mechanisms and functions of spontaneous neurotransmitter release. Nature Reviews Neuroscience. 2015; 16(1):5–16. [PubMed: 25524119]

Khakh BS. ATP-gated P2X receptors on excitatory nerve terminals onto interneurons initiate a form of asynchronous glutamate release. Neuropharmacology. 2009; 56(1):216–222. [PubMed: 18601937]

Kombian SB, Hirasawa M, Mouginot D, Chen X, Pittman QJ. Short-term potentiation of miniature excitatory synaptic currents causes excitation of supraoptic neurons. Journal of Neurophysiology. 2000; 83(5):2542–2553. [PubMed: 10805656]

Krizaj D, Bao JX, Schmitz Y, Witkovsky P, Copenhagen DR. Caffeine-sensitive calcium stores regulate synaptic transmission from retinal rod photoreceptors. The Journal of Neuroscience. 1999; 19(17):7249–7261. [PubMed: 10460231]

Lai Y, Diao J, Cipriano DJ, Zhang Y, Pfuetzner RA, Padolina MS, Brunger AT. Complexin inhibits spontaneous release and synchronizes Ca^{2+}-triggered synaptic vesicle fusion by distinct mechanisms. Elife. 2014; 3:e03756. [PubMed: 25122624]

Larsson HP, Picaud SA, Werblin FS, Lecar H. Noise analysis of the glutamate-activated current in photoreceptors. Biophysical Journal. 1996; 70(2):733–742. [PubMed: 8789090]

Lasansky A. Contacts between receptors and electrophysiologically identified neurones in the retina of the larval tiger salamander. The Journal of Physiology. 1978; 285:531–542. [PubMed: 217992]

Llinás RR. Depolarization release coupling: an overview. Annals of the New York Academy of Sciences. 1991; 635:3–17. [PubMed: 1660239]

Lou X, Scheuss V, Schneggenburger R. Allosteric modulation of the presynaptic Ca^{2+} sensor for vesicle fusion. Nature. 2005; 435:497–501. [PubMed: 15917809]

Maple BR, Werblin FS, Wu SM. Miniature excitatory postsynaptic currents in bipolar cells of the tiger salamander retina. Vision Research. 1994; 34(18):2357–2362. [PubMed: 7975276]

Maxeiner S, Luo F, Tan A, Schmitz F, Südhof TC. How to make a synaptic ribbon: RIBEYE deletion abolishes ribbons in retinal synapses and disrupts neurotransmitter release. The EMBO Journal. 2016:e201592701.

Maximov A, Tang J, Yang X, Pang ZP, Südhof TC. Complexin controls the force transfer from SNARE complexes to membranes in fusion. Science. 2009; 323:516–521. [PubMed: 19164751]

McKinney RA, Capogna M, Dürr R, Gähwiler BH, Thompson SM. Miniature synaptic events maintain dendritic spines via AMPA receptor activation. Nature Neuroscience. 1999; 2(1):44–49. [PubMed: 10195179]

Mehta B, Snellman J, Chen S, Li W, Zenisek D. Synaptic ribbons influence the size and frequency of miniature-like evoked postsynaptic currents. Neuron. 2013; 77(3):516–527. [PubMed: 23395377]

Melom JE, Akbergenova Y, Gavornik JP, Littleton JT. Spontaneous and evoked release are independently regulated at individual active zones. The Journal of Neuroscience. 2013; 33(44): 17253–17263. [PubMed: 24174659]

Mercer AJ, Rabl K, Riccardi GE, Brecha NC, Stella SL Jr, Thoreson WB. Location of release sites and calcium-activated chloride channels relative to calcium channels at the photoreceptor ribbon synapse. Journal of Neurophysiology. 2011; 105(1):321–335. [PubMed: 21084687]

Morgans CW. Localization of the alpha(1F) calcium channel subunit in the rat retina. Investigative Ophthalmology & Visual Science. 2001; 42(10):2414–2418. [PubMed: 11527958]

Murthy VN, Stevens CF. Reversal of synaptic vesicle docking at central synapses. Nature Neuroscience. 1999; 2:503–507. [PubMed: 10448213]

Nachman-Clewner M, St Jules R, Townes-Anderson E. L-type calcium channels in the photoreceptor ribbon synapse: localization and role in plasticity. Journal of Comparative Neurology. 1999; 415(1):1–16. [PubMed: 10540354]

Pang ZP, Bacaj T, Yang X, Zhou P, Xu W, Südhof TC. Doc2 supports spontaneous synaptic transmission by a Ca(2+)-independent mechanism. Neuron. 2011; 70(2):244–251. [PubMed: 21521611]

Pedersen UR, Leidy C, Westh P, Peters GH. The effect of calcium on the properties of charged phospholipid bilayers. Biochimica et Biophysica Acta. 2006; 1758(5):573–582. [PubMed: 16730642]

Peled ES, Newman ZL, Isacoff EY. Evoked and spontaneous transmission favored by distinct sets of synapses. Current Biology. 2014; 24(5):484–493. [PubMed: 24560571]

Peters JH, McDougall SJ, Fawley JA, Smith SM, Andresen MC. Primary afferent activation of thermosensitive TRPV1 triggers asynchronous glutamate release at central neurons. Neuron. 2010; 65:657–669. [PubMed: 20223201]

Picaud S, Larsson HP, Wellis DP, Lecar H, Werblin F. Cone photoreceptors respond to their own glutamate release in the tiger salamander. Proceedings of the National Academy of Sciences. 1995; 92(20):9417–9421.

Piccolino M, Byzov AL, Kurennyi DE, Pignatelli A, Sappia F, Wilkinson M, Barnes S. Low-calcium-induced enhancement of chemical synaptic transmission from photoreceptors to horizontal cells in the vertebrate retina. Proceedings of the National Academy of Sciences. 1996; 93(6):2302–2306.

Piccolino M, Pignatelli A. Calcium-independent synaptic transmission: artifact or fact? Trends in Neuroscience. 1996; 19(4):120–125.

Piccolino M, Vellani V, Rakotobe LA, Pignatelli A, Barnes S, McNaughton P. Manipulation of synaptic sign and strength with divalent cations in the vertebrate retina: pushing the limits of tonic, chemical neurotransmission. Eur J Neurosci. 1999; 11(11):4134–4138. [PubMed: 10583501]

Ramirez DM, Khvotchev M, Trauterman B, Kavalali ET. Vti1a identifies a vesicle pool that preferentially recycles at rest and maintains spontaneous neurotransmission. Neuron. 2012; 73:121–134. [PubMed: 22243751]

Rao-Mirotznik R, Buchsbaum G, Sterling P. Transmitter concentration at a three-dimensional synapse. Journal of Neurophysiology. 1998; 80(6):3163–3172. [PubMed: 9862914]

Rea R, Li J, Dharia A, Levitan ES, Sterling P, Kramer RH. Streamlined synaptic vesicle cycle in cone photoreceptor terminals. Neuron. 2004; 41(5):755–766. [PubMed: 15003175]

Rhee JS, Li LY, Shin OH, Rah JC, Rizo J, Südhof TC, Rosenmund C. Augmenting neurotransmitter release by enhancing the apparent Ca^{2+} affinity of synaptotagmin 1. Proceedings of the National Academy of Sciences. 2005; 102(51):18664–18669.

Rost BR, Schneider F, Grauel MK, Wozny C1, G Bentz C, Blessing A, Rosenmund T, Jentsch TJ, Schmitz D, Hegemann P, Rosenmund C. Optogenetic acidification of synaptic vesicles and lysosomes. Nature Neuroscience. 2015; 18(12):1845–1852. [PubMed: 26551543]

Rowan MJ, Ripps H, Shen W. Fast glutamate uptake via EAAT2 shapes the cone-mediated light offset response in bipolar cells. The Journal of Physiology. 2010; 588(Pt 20):3943–3956. [PubMed: 20807794]

Sara Y, Virmani T, Deák F, Liu X, Kavalali ET. An isolated pool of vesicles recycles at rest and drives spontaneous neurotransmission. Neuron. 2005; 45(4):563–573. [PubMed: 15721242]

Scanziani M, Capogna M, Gahwiler BH, Thompson SM. Presynaptic inhibition of miniature excitatory synaptic currents by baclofen and adenosine in the hippocampus. Neuron. 1992; 9:919–927. [PubMed: 1358131]

Scheuber A, Rudge R, Danglot L, Raposo G, Binz T, Poncer JC, Galli T. Loss of AP-3 function affects spontaneous and evoked release at hippocampal mossy fiber synapses. Proceedings of the National Academy of Sciences. 2006; 103(44):16562–16567.

Schneggenburger R, Rosenmund C. Molecular mechanisms governing Ca(2+) regulation of evoked and spontaneous release. Nature Neuroscience. 2015; 18(7):935–941. [PubMed: 26108721]

Schneider R, Hosy E, Kohl J, Klueva J, Choquet D, Thomas U, Voigt A, Heine M. Mobility of calcium channels in the presynaptic membrane. Neuron. 2015; 86(3):672–679. [PubMed: 25892305]

Schweizer FE, Ryan TA. The synaptic vesicle: cycle of exocytosis and endocytosis. Current Opinion in Neurobiology. 2006; 16(3):298–304. [PubMed: 16707259]

Shoudai K, Peters JH, McDougall SJ, Fawley JA, Andresen MC. Thermally active TRPV1 tonically drives central spontaneous glutamate release. The Journal of Neuroscience. 2010; 30:14470–14475. [PubMed: 20980604]

Smith SM, Chen W, Vyleta NP, Williams C, Lee CH, Phillips C, Andresen MC. Calcium regulation of spontaneous and asynchronous neurotransmitter release. Cell Calcium. 2012; 52(3-4):226–233. [PubMed: 22748761]

Snellman J, Mehta B, Babai N, Bartoletti TM, Akmentin W, Francis A, Matthews G, Thoreson W, Zenisek D. Acute destruction of the synaptic ribbon reveals a role for the ribbon in vesicle priming. Nature Neuroscience. 2011; 14(9):1135–1141. [PubMed: 21785435]

Sun J, Pang ZP, Qin D, Fahim AT, Adachi R, Südhof TC. A dual-Ca^{2+}-sensor model for neurotransmitter release in a central synapse. Nature. 2007; 450:676–682. [PubMed: 18046404]

Suryanarayanan A, Slaughter MM. Synaptic transmission mediated by internal calcium stores in rod photoreceptors. The Journal of Neuroscience. 2006; 26(6):1759–1766. [PubMed: 16467524]

Sutton MA, Ito HT, Cressy P, Kemp AC, Woo JC, Schuman EM. Miniature neurotransmission stabilizes synaptic function via tonic suppression of local dendritic protein synthesis. Cell. 2006; 125(4):785–799. [PubMed: 16713568]

Szmajda BA, Devries SH. Glutamate spillover between mammalian cone photoreceptors. The Journal of Neuroscience. 2011; 31(38):13431–13441. [PubMed: 21940436]

Thoreson WB, Rabl K, Townes-Anderson E, Heidelberger R. A highly Ca^{2+}-sensitive pool of vesicles contributes to linearity at the rod photoreceptor ribbon synapse. Neuron. 2004; 42(4):595–605. [PubMed: 15157421]

Thoreson WB, Stella SL Jr, Bryson EI, Clements J, Witkovsky P. D2-like dopamine receptors promote interactions between calcium and chloride channels that diminish rod synaptic transfer in the salamander retina. Visual Neuroscience. 2002; 19(3):235–247. [PubMed: 12392173]

Thoreson WB, Van Hook MJ, Parmelee C, Curto C. Modeling and measurement of vesicle pools at the cone ribbon synapse: Changes in release probability are solely responsible for voltage-dependent changes in release. Synapse. 2016; 70(1):1–14. [PubMed: 26541100]

Traynelis SF, Wollmuth LP, McBain CJ, Menniti FS, Vance KM, Ogden KK, Hansen KB, Yuan H, Myers SJ, Dingledine R. Glutamate receptor ion channels: structure, regulation, and function. Pharmacological Reviews. 2010; 62(3):405–496. [PubMed: 20716669]

Vaithianathan T, Henry D, Akmentin W, Matthews G. Nanoscale dynamics of synaptic vesicle trafficking and fusion at the presynaptic active zone. Elife. 2016:e13245. [PubMed: 26880547]

Vaithianathan T, Henry D, Akmentin W, Matthews G. Functional roles of complexin in neurotransmitter release at ribbon synapses of mouse retinal bipolar neurons. The Journal of Neuroscience. 2015; 35(9):4065–4070. [PubMed: 25740533]

Vaithianathan T, Zanazzi G, Henry D, Akmentin W, Matthews G. Stabilization of spontaneous neurotransmitter release at ribbon synapses by ribbon-specific subtypes of complexin. The Journal of Neuroscience. 2013; 33(19):8216–8226. [PubMed: 23658160]

Vandenbranden CA, Yazulla S, Studholme KM, Kamphuis W, Kamermans M. Immunocytochemical localization of the glutamate transporter GLT-1 in goldfish (Carassius auratus) retina. Journal of Comparative Neurology. 2000; 423(3):440–451. [PubMed: 10870084]

Van Hook MJ, Thoreson WB. Simultaneous whole-cell recordings from photoreceptors and second-order neurons in an amphibian retinal slice preparation. Journal of Visualized Experiments. 2013; (76)

Van Hook MJ, Thoreson WB. Weak endogenous Ca^{2+} buffering supports sustained synaptic transmission by distinct mechanisms in rod and cone photoreceptors in salamander retina. Physiological Reports. 2015; 3(9) pii: e12567.

Vyleta NP, Smith SM. Spontaneous glutamate release is independent of calcium influx and tonically activated by the calcium-sensing receptor. The Journal of Neuroscience. 2011; 31:4593–4606. [PubMed: 21430159]

Weber JP, Reim K, Sørensen JB. Opposing functions of two sub-domains of the SNARE-complex in neurotransmission. The EMBO Journal. 2010; 29:2477–2490. [PubMed: 20562829]

Williams C, Chen W, Lee CH, Yaeger D, Vyleta NP, Smith SM. Coactivation of multiple tightly coupled calcium channels triggers spontaneous release of GABA. Nature Neuroscience. 2012; 15:1195–1197. [PubMed: 22842148]

Xu J, Pang ZP, Shin OH, Südhof TC. Synaptotagmin-1 functions as a Ca^{2+} sensor for spontaneous release. Nature Neuroscience. 2009; 12(6):759–766. [PubMed: 19412166]

Zampighi GA, Schietroma C, Zampighi LM, Woodruff M, Wright EM, Brecha NC. Conical tomography of a ribbon synapse: structural evidence for vesicle fusion. PLoS One. 2011; 6(3):e16944. [PubMed: 21390245]

Zenisek D. Vesicle association and exocytosis at ribbon and extraribbon sites in retinal bipolar cell presynaptic terminals. Proceedings of the National Academy of Sciences. 2008; 105(12):4922–4927.

Zenisek D, Horst NK, Merrifield C, Sterling P, Matthews G. Visualizing synaptic ribbons in the living cell. The Journal of Neuroscience. 2004; 24(44):9752–9759. [PubMed: 15525760]

Zhang AJ, Zhang J, Wu SM. Electrical coupling, receptive fields, and relative rod/cone inputs of horizontal cells in the tiger salamander retina. Journal of Comparative Neurology. 2006; 499(3): 422–431. [PubMed: 16998920]

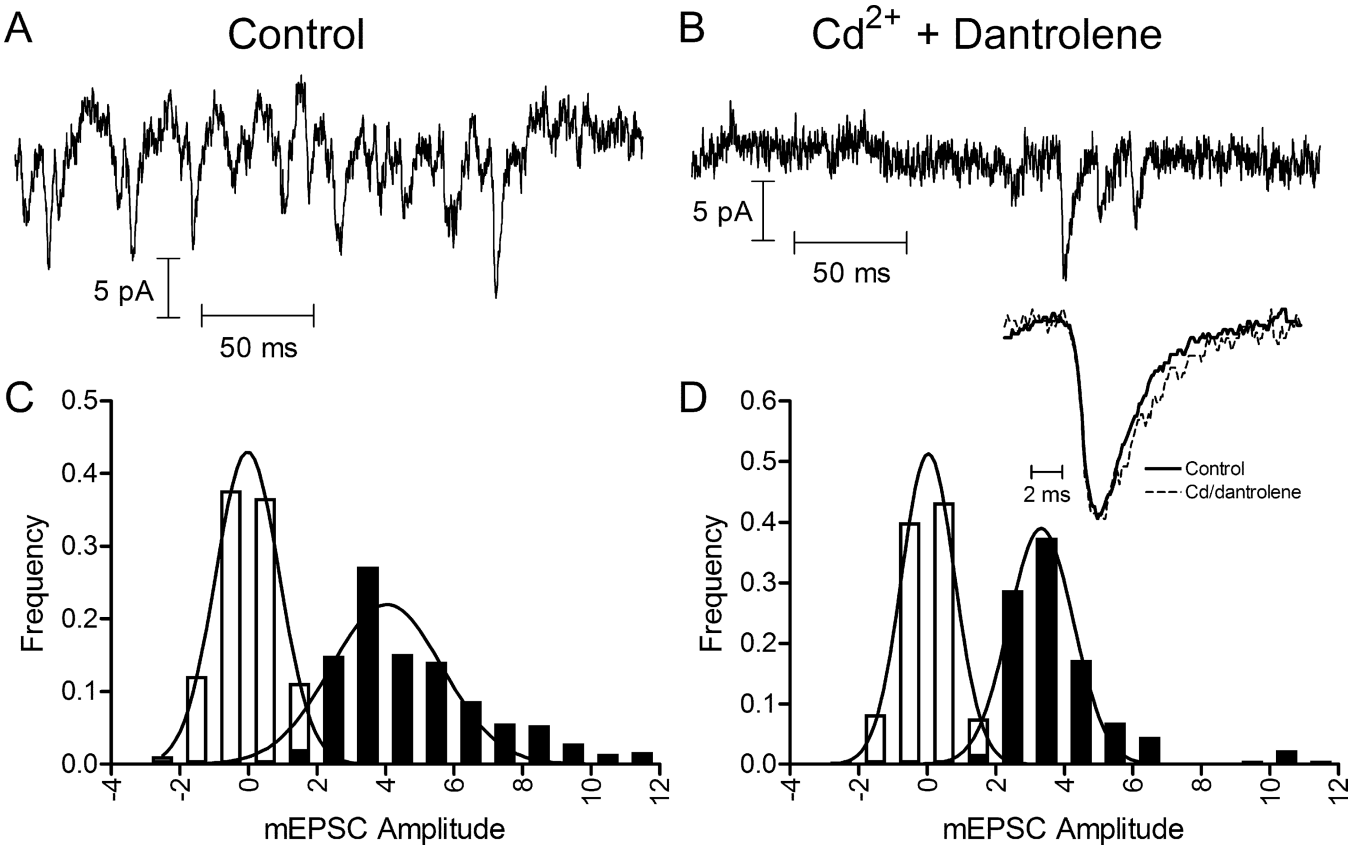

Figure 1.

mEPSCs persisted after blocking Ca^{2+} channels with Cd^{2+} (100 μM) and CICR with dantrolene (10 μM). mEPSCs were measured by whole-cell patch clamp recording in horizontal cells (HCs). Representative traces show mEPSCs in control conditions **(A)** and following application of Cd^{2+} plus dantrolene in the same cell **(B). (C)** and **(D)** show mEPSC amplitude histograms from the same cell. The filled bars show event histograms and open bars show baseline noise histograms. Distributions were fit with Gaussian curves. Control data (**C** ; 482 events) were fit with a mean amplitude of 4.03 pA and standard deviation of 1.63 pA. Cd^{2+} plus dantrolene data (**D** ; 174 events) were fit with a mean amplitude of 3.33 pA and standard deviation of 0.94 pA. Inset shows average waveforms for well-isolated mEPSCs in control (N = 50 events) and Cd^{2+} plus dantrolene (N = 26) conditions. Waveforms were normalized to their peak amplitudes.

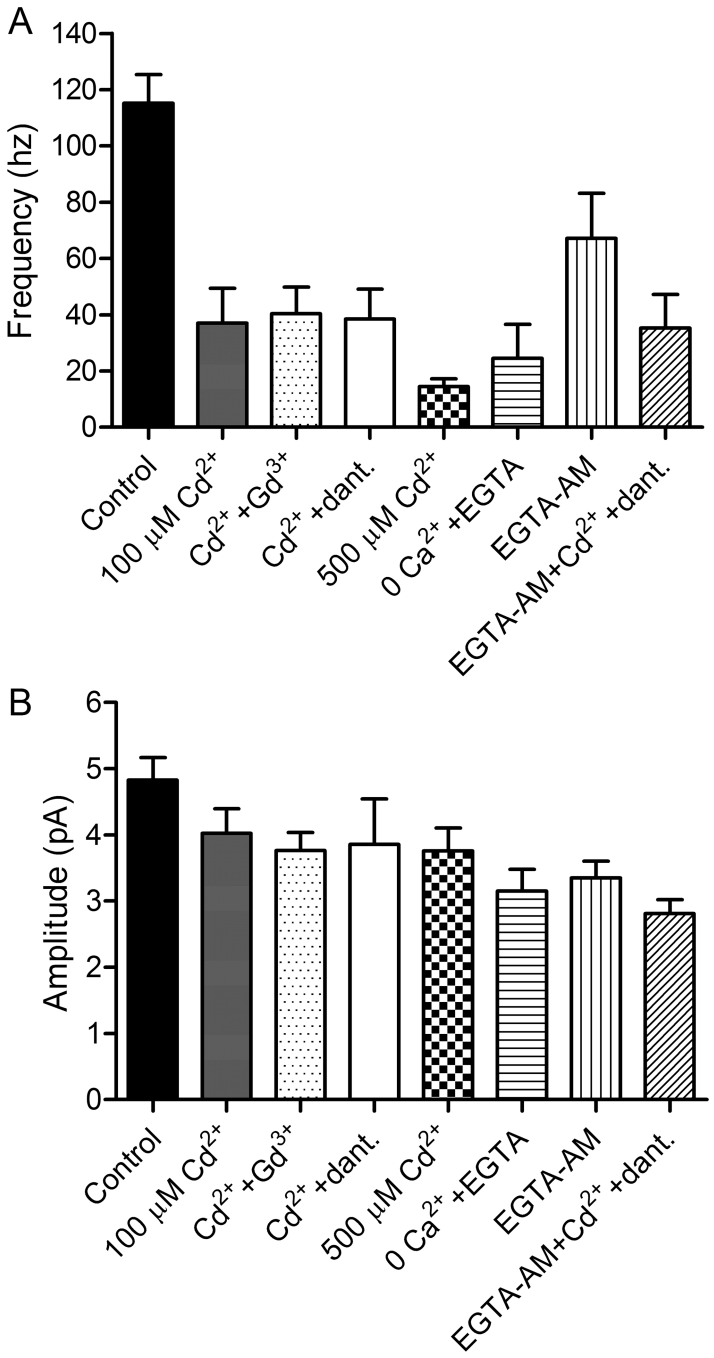

Figure 2.

HC mEPSCs were reduced in frequency but not abolished when Ca^{2+} influx was inhibited. mEPSCs were recorded in HCs voltage clamped at −60 mV. **(A)** HC mEPSCs in control conditions had a frequency of 115.2 ± 10.1 (N = 28 HCs). Application of Cd^{2+} (100 μM) reduced the frequency of mEPSCs to 37.0 ± 12.4 Hz (N = 8 HCs). Cd^{2+} (100 μM) plus Gd^{3+} (30 μM) reduced the frequency to 40.5 ± 9.4 Hz (N = 7 HCs). Cd^{2+} (100 μM) plus dantrolene (10 μM) reduced the frequency to 38.5 ± 10.7 Hz (N = 11 HCs). A higher concentration of Cd^{2+} (500 μM) caused a somewhat greater reduction (14.5 ± 2.7 Hz, N=8;

median = 15.8 Hz; P = 0.078 compared to Cd^{2+} plus dantrolene, unpaired t-test). In Ca^{2+}-free extracellular solution with EGTA (1 mM), mEPSCs had a frequency of 24.5 ± 6.28 Hz (N = 5 HCs). After incubating retinas in EGTA-AM (100 μM) for 2 hours, the frequency of mEPSCs was reduced to 67.2 ± 16.0 Hz, N = 10 HCs). Addition of Cd^{2+} plus dantrolene to slices incubated in EGTA-AM reduced mEPSC frequency to 35.3 ± 12.0 Hz (N = 9 HCs). Frequencies in all of these conditions were significantly lower than control conditions ($P<0.05$ for EGTA-AM, $P < 0.001$ for all other comparisons, Bonferroni's multiple comparison test). With the exception of 0 Ca^{2+} plus EGTA (P = 0.113), frequencies of all conditions were significantly non-zero ($P < 0.005$, one-sided t-tests). **(B)** In control conditions, mEPSCs had an amplitude of 4.8 ± 0.34 pA (N = 28 HCs). Event amplitudes averaged: 100 μM Cd^{2+} (4.0 ± 0.37 pA, N=8), 100 μM Cd^{2+} plus 30 μM Gd^{3+} (3.8 ± 0.27 pA, N=7), 100 μM Cd^{2+} plus dantrolene (3.9 ± 0.68 pA, N=11), 500 μM Cd^{2+} (3.8 ± 0.35 pA, N=8), 0 Ca^{2+} plus 1 mM EGTA (3.2 ± 0.33 pA, N=5), EGTA-AM (3.4 ± 0.26 pA, N=9), and EGTA-AM plus 100 μM Cd^{2+} and dantrolene (2.8 ± 0.21 pA, N=9). The amplitude of spontaneous release events measured in the presence of these various blockers were not significantly smaller than control ($P > 0.05$, Bonferroni's multiple comparison test) with the exception of EGTA-AM plus 100 μM Cd^{2+} ($P < 0.01$).

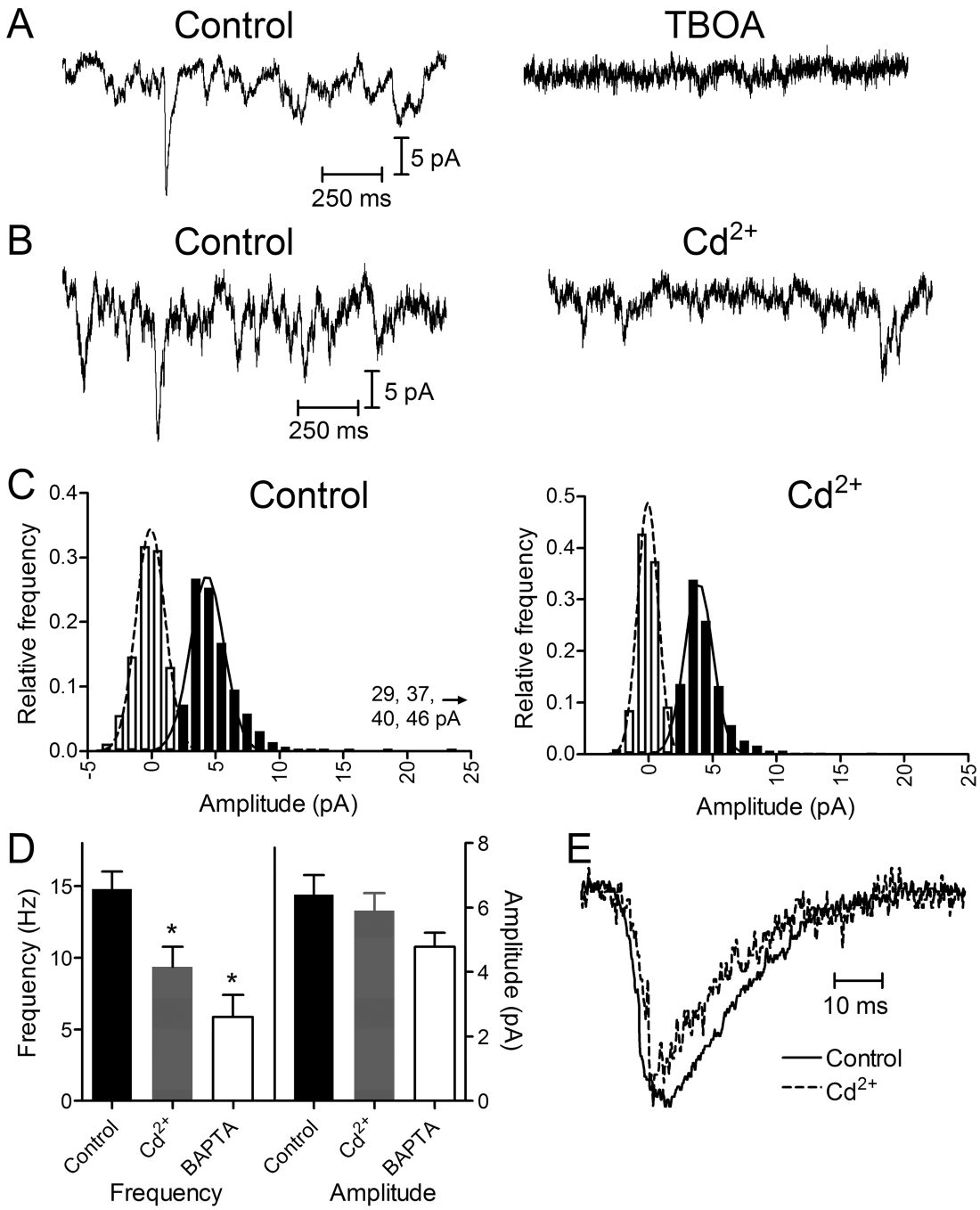

Figure 3.

Presynaptic release events detected in rods by glutamate transporter anion currents. **(A)** Presynaptic quantal transporter currents in rods voltage clamped at −70 mV were blocked by inhibiting the glutamate transporter with TBOA (100 μM). **(B)** Representative trace from an individual rod before and after application of Cd^{2+} (100 μM) showing a reduction in the frequency of presynaptic events. **(C)** Amplitude histograms of release events from the same rod in control and Cd^{2+}. The filled bars show event histograms and open bars show baseline noise histograms. Distributions were fit with Gaussian curves. Control data (291 events)

were fit with a mean amplitude of 5.54 pA and standard deviation of 4.57 pA. Cd^{2+} data (301 events) were fit with a mean amplitude of 4.54 pA and standard deviation of 2.64 pA. The ordinate was plotted to 25 pA, but four events with larger amplitudes of 29, 37, 40 and 46 pA were also observed in control conditions. (D) Bar graph illustrating frequency and amplitudes of rod presynaptic events in control (14.8 ± 1.2 Hz, 6.42 ± 0.48 pA, N = 23), Cd^{2+} (100 μM; 9.35 ± 1.4 Hz, 5.90 ± 0.55 pA, N = 13), and after introduction of 10 mM BAPTA into the rod through a patch pipette (5.86 ± 1.5 Hz, 4.78 ± 0.43 pA, N = 9). Reduction in frequency with Cd^{2+} (paired t-test, N=12 pairs, P = 0.0011) and BAPTA (unpaired t-test, P = 0.0003) were both significant relative to control. (E) Average waveforms for well-isolated rod transporter currents in control (N = 42 events) and Cd^{2+} (N = 28) conditions. Waveforms were normalized to their peak amplitudes.

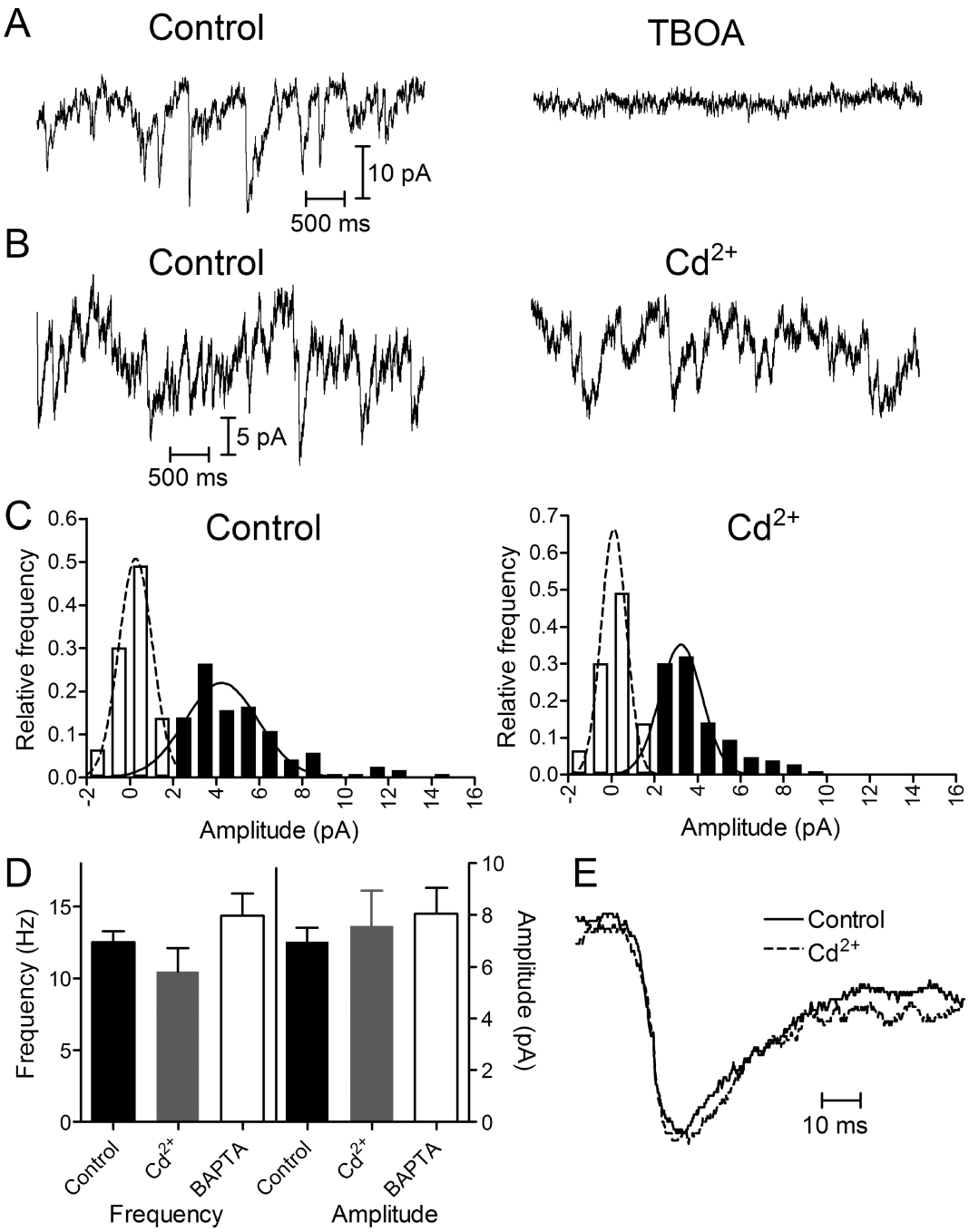

Figure 4.

Presynaptic release events detected in cones by glutamate transporter anion currents. **(A)** Presynaptic quantal transporter currents in cones voltage clamped at −70 mV were blocked by inhibiting the glutamate transporter with TBOA (100 μM). **(B)** Cone transporter currents before and after application of Cd^{2+} (100 μM). **(C)** Amplitude histograms of release events from the same cone in control and Cd^{2+}. Filled bars show event histograms and open bars show baseline noise histograms. Distributions were fit with Gaussian curves. Control data (121 events) were fit with a mean amplitude of 4.26 pA and standard deviation of 1.69 pA.

Cd^{2+} data (106 events) were fit with a mean amplitude of 3.23 pA and standard deviation of 0.97 pA. **(D)** Bar graph illustrating frequency and amplitudes of rod presynaptic events in control (12.5 ± 0.77 Hz, 6.96 ± 0.55 pA, N = 6), Cd^{2+} (100 μM; 10.5 ± 1.6 Hz, 7.57 ± 1.38 pA, N = 6), and after introduction of 10 mM BAPTA into the cone through a patch pipette (14.4 ± 1.5 Hz, 8.03 ± 1.01 pA, N = 7). Changes in frequency and amplitude with Cd^{2+} or BAPTA were not significant relative to control (paired t-tests comparing Cd^{2+} and control; also Bonferroni's multiple comparison test). **(E)** Average waveforms for well-isolated cone transporter currents in control (N = 53) and Cd^{2+} (N = 36) conditions. Waveforms were normalized to their peak amplitudes.

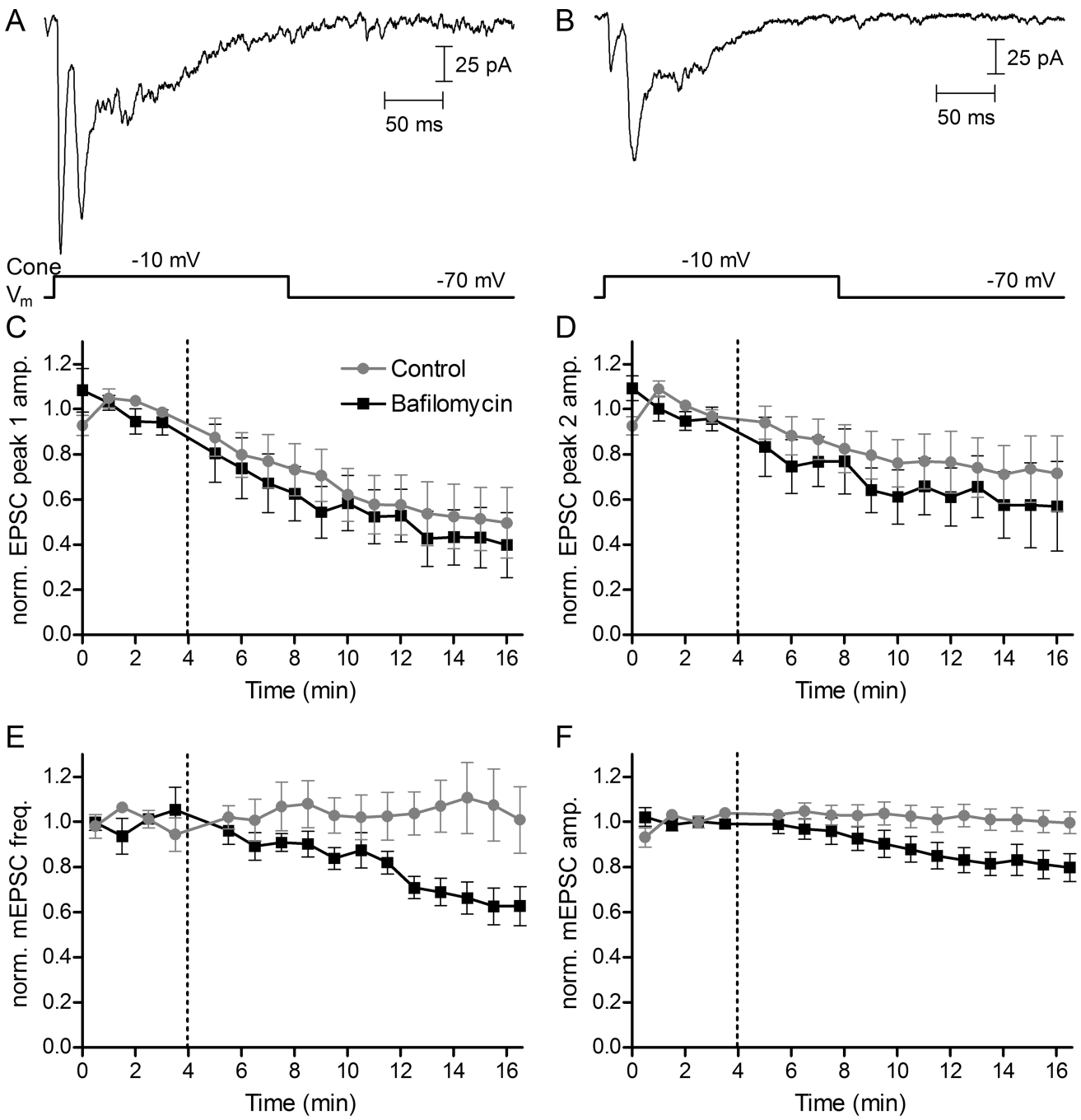

Figure 5.

Using the vesicular ATPase inhibitor bafilomycin to block refilling of vesicles with glutamate caused different rates of decline in EPSCs and mEPSCs. **(A)** A representative EPSC in control conditions evoked in an HC by a 200-ms depolarizing step from −70 to −10 mV applied to a simultaneously voltage-clamped rod. The depolarizing step evoked an initial fast EPSC due to release from ribbons followed by a second slower peak due to non-ribbon release (Chen et al., 2014). **(B)** An EPSC evoked in the same rod/HC pair 15 min after application of bafilomycin (7 μM) showed a decrease in amplitude of both EPSC peaks.

(C) EPSC amplitude and mEPSC frequency and amplitude were normalized to the average of four responses obtained prior to bafilomycin application at 4 minutes (dashed vertical lines). The 1st and 2nd EPSC peaks both declined in control conditions due to rundown. The declines in amplitude of the 1st **(C)** and 2nd **(D)** EPSC peaks were accelerated slightly but not significantly by bafilomycin (comparing the change in normalized EPSC amplitude of the first 3 vs. last 3 responses from rod/HC pairs in control N=9 vs. bafilomycin N=8: peak 1, P = 0.65; peak 2, P=0.44, unpaired t-tests). In contrast to changes in EPSC amplitude, HC mEPSC frequency **(E)** and amplitude **(F)** both declined significantly during application of bafilomycin (average of the first 3 vs. last 3 records in control vs. bafilomycin, frequency: $P < 0.04$; amplitude: $P < 0.04$; N = 7 HCs in bafilomycin, N = 8 HCs in control, unpaired t-tests). HC mEPSCs were collected in 10 s trials in which the rod was voltage clamped at −70 mV. EPSC and mEPSC trials alternated every 30 s.

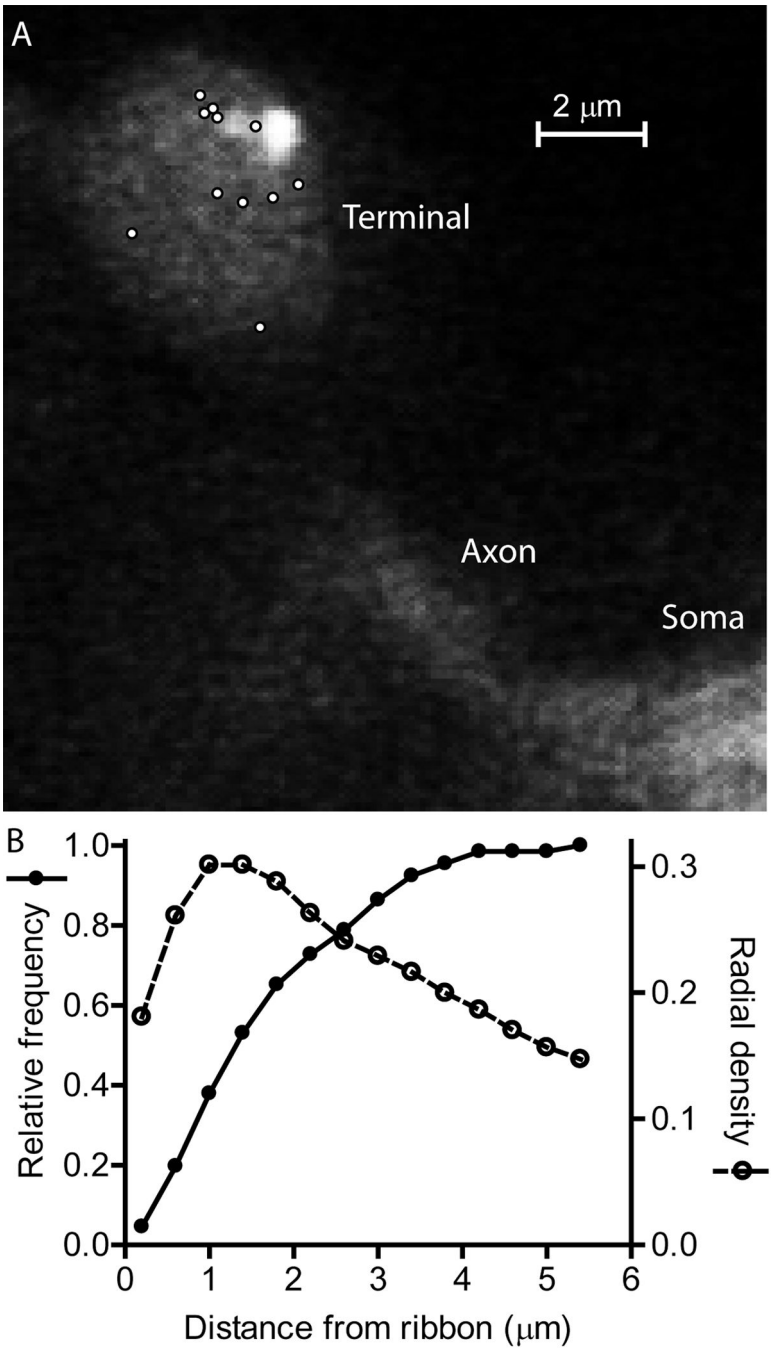

Figure 6.

Locations of individual spontaneous release events and synaptic ribbons visualized by TIRF microscopy. **(A)** A representative rod terminal with sites of individual spontaneous release events indicated by white circles. The elliptical footprint of the synaptic terminal membrane as well as some of the axon and soma emitted a faint fluorescent glow (525 nm emission) when excited with the 488 nm laser. One can also see two neighboring ribbons labeled with fluorescent Hylite488-conjugated ribeye-binding peptide (80 μM) in the upper right portion of the terminal. To detect release events, synaptic vesicles were loaded with 10 kD dextran-

conjugated pHrodo loaded and visualized with 561 nm excitation/609 nm emission. Ca^{2+}-independent spontaneous release events were measured in isolated rods voltage clamped at −70 mV in the presence of Cd^{2+} (100 μM) plus dantrolene (10 μM). **(B)** The relative frequency of Ca^{2+}-independent spontaneous release events at different distances from the synaptic ribbon. The distance between individual release events and the center of the nearest ribbon averaged 1.80 ± 0.14 μm (N = 66 events in 9 rods). We calculated the radial density distribution of events, d(r), using the following formula $d(r) = N(r)/\pi[(r + n/2)^2 – (r - n/2)^2]$ where r is the radial distance to the center of each bin in the histogram from the center of the nearest ribbon, n is the width of each bin (400 nm), and N(r) is the number of events in each bin. A sizable percentage of release events (>60%), occurred more than 1 μm away from the nearest synaptic ribbon, but the highest density of events occurred 1–1.4 μm from the nearest ribbon.